Scientific Research and Essays

Volume 10 Number 2 30 January 2015
ISSN 1992-2248

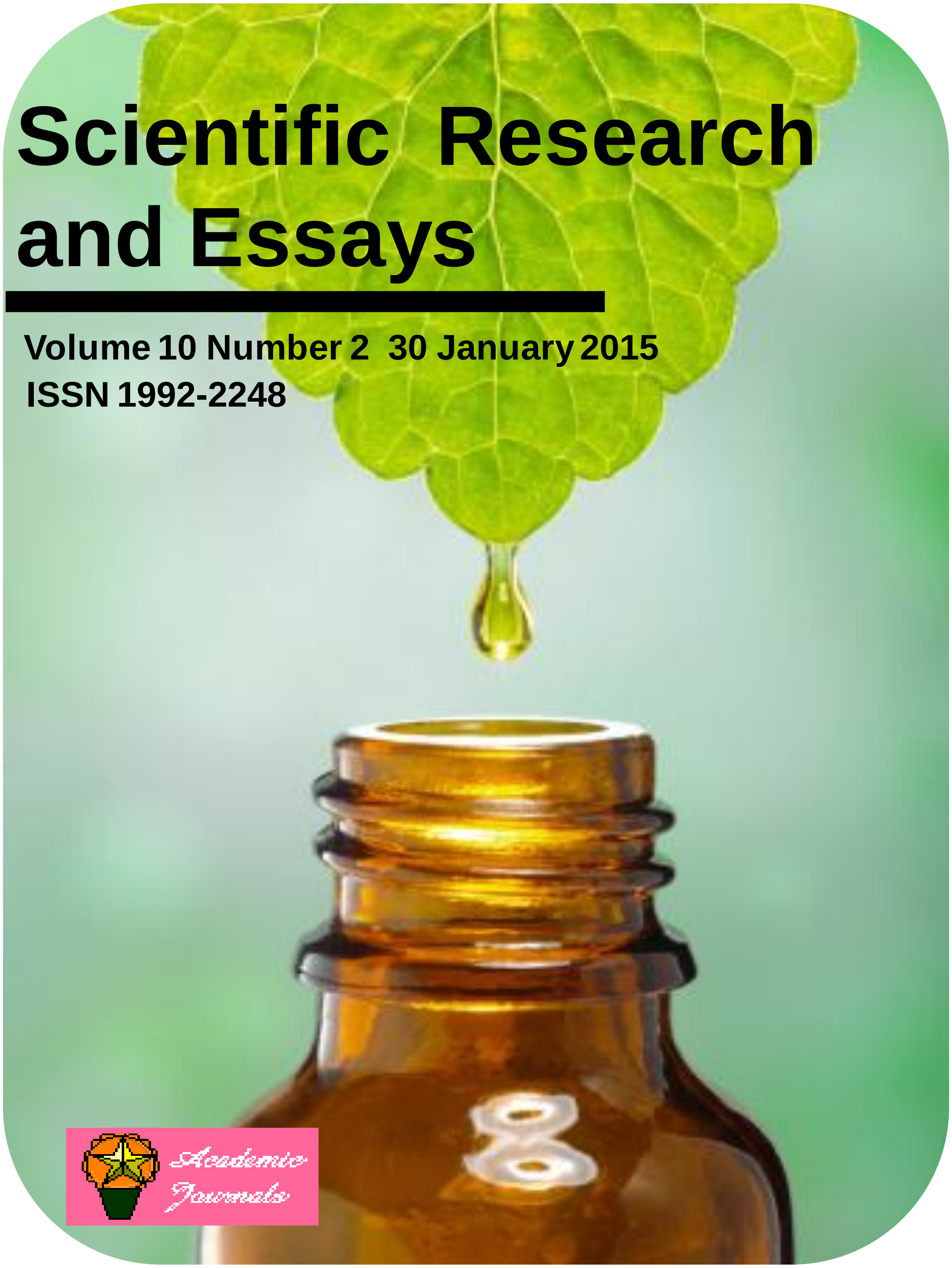

Academic Journals

ABOUT SRE

The **Scientific Research and Essays (SRE)** is published twice monthly (one volume per year) by Academic Journals.

Scientific Research and Essays (SRE) is an open access journal with the objective of publishing quality research articles in science, medicine, agriculture and engineering such as Nanotechnology, Climate Change and Global Warming, Air Pollution Management and Electronics etc. All papers published by SRE are blind peer reviewed.

SubmissionofManuscript

Submit manuscripts as email attachment to the Editorial Office at sre@academicjournals.org. A manuscript number will be mailed to the corresponding author shortly after submission.

The Scientific Research and Essays will only accept manuscripts submitted as e-mail attachments.

Please read the **Instructions for Authors** before submitting your manuscript. The manuscript files should be given the last name of the first author.

Editors

EditorialBoard

Fees andCharges:Authorsarerequired topay a$550handlingfee.Publicationofanarticlein theScientific ResearchandEssaysisnotcontingentupontheauthor'sabilitytopaythecharges.Neitherisacceptancetopaythehandlingfeea guaranteethatthepaperwillbeacceptedforpublication.Authorsmaystillrequest(inadvance)thattheeditorialofficewaiveso meofthe handlingfeeunder specialcircumstances.

ScientificResearchandEssays

Table of Contents: Volume 10 Number 2 30 January, 2015

ARTICLES

Research Articles

Manuel Antonio Bouzas Sanchis, André Luiz Severiano Câmara,
João Paulo da Silva Gonçalo and Andrei de Abiahy Carneiro da Cunha Braga

academicJournals

Vol. 10(2), pp. 41-52, 30 January, 2015
DOI: 10.5897/SRE2014.5831
Article Number: D9EAA2649787
ISSN 1992-2248
Copyright©2015
Author(s) retain the copyright of this article
http://www.academicjournals.org/SRE

Scientific Research and Essays

Full Length Research Paper

Laminar free and forced convection cooling of a semi permeable open cavity

C. A. Chaves[1*], W. Q. Lamas[2], J. R. Camargo[1], F. J. Grandinetti[1], C. A. C. Altemani[3]

[1]Mechanical Engineering Department, University of Taubaté, Rua Daniel Danelli, s/nº - Jardim Morumbí 12060-440 - Taubaté - SP - Brazil.
[2]Mechanical Engineering Department and Department of Basic and Environmental Sciences (School of Engineering at Lorena), University of Taubaté and University of Sao Paulo, Brazil.
[3]Mechanical Engineering Department, University of Campinas - Campinas - SP - Brazil.

Received 5 February, 2014; Accepted 19 January, 2015

Heat transfer inside a semi porous two-dimensional rectangular open cavity was numerically investigated. The open cavity comprises two vertical walls closed to the bottom by an adiabatic horizontal wall. One vertical wall is a porous and an inflow of fluid occurs normal to it. The other wall transfers a uniform heat flux to the cavity. It shows how natural convection effects may enhance the forced convection inside the open cavity. The main motivation for the work is its application for electronic equipment where frequently the devices used for the electronic equipment cooling are based on natural and forced convection. Governing equations are expressed in Cartesian coordinates and numerically handled by a finite volume method. Results are presented for both local and average Nusselt numbers at the heated wall and for the isotherms and streamlines of the fluid flowing inside the open cavity as a function of Reynolds number ranging from 1 to 100, Grashof number ranging from 0 to 10^{+7} and the aspect ratio number of the open cavity equal 2, 4 and 8. The results obtained show that the forced convection inside the semi-porous open cavity studied may be greatly enhanced by natural convection effects.

Key words: Computational simulation, electronic equipment cooling, finite volume, natural convection, open cavity; porous media.

INTRODUCTION

The heat transfer in enclosures has been studied for a variety of engineering applications. Results have been presented in research surveys (Bruchberg et al., 1976; Kakaç et al., 1987) and it has become a main topic in convective heat transfer textbooks (Bejan, 1984). Usually the enclosures are closed and natural convection is the single heat transfer mechanism. There are however, several applications in passive solar heating, energy conservation in building and cooling of electronic equipment, where open cavities are employed (Chan and Tien, 1985; Hess and Henze, 1984; Penot, 1982).

Frequently the devices employed for the cooling of electronic equipment are based on forced convection (Sparrow et al., 1985). Studies on Computational Fluid Dynamics (CFD) applied to analysis of electronics cooling had been developed in several works. Specially theory

*Corresponding author email: carlos.chaves@unitau.br, Tel/Fax: +55 12 3621-8002.

on natural convection in enclosures (Ostrach, 1972) and electronics cooling enclosure used as part of a larger telecommunication radar system (Boukhanouf and Haddad, 2010). Also studies of flow characteristics are done numerically with CFD and compared to experimental approaches, that is, manifolds that are widely used in electronic cooling equipment (Gandhi et al., 2012), shielded heat sink also widely used in that (Shaalan et al., 2012), and analysis to eliminate fan used in electronic device cooling (Nickell, 1997).

Several studies on natural convection in open cavities had been done. Steady-state natural convection taking place in rectangular cavities filled with air was studied both experimental and numerically in Bairi et al. (2007). A steady buoyancy-driven flow of air in a partially open square 2D cavity with internal heat source, adiabatic bottom and top walls, and vertical walls maintained at different constant temperatures was investigated numerically in Fontana et al. (2011). The numerical results of heat transfer calculations in an open cavity considering natural convection and temperature-dependent fluid properties were presented by Juarez et al. (2011). The natural convection occurring from open cavities was analysed by Prakash et al. (2012) in three different cavity shapes namely cubical, spherical and hemispherical geometries having equal heat transfer area. The thermal behaviour of airborne electronic equipment submitted to natural convection in closed parallelogrammic air-filled cavities was examined by Bairi et al. (2012). Also mixed convection in open cavity had been reviewed through several works.

Wong and Saeid (2009) investigated the opposing mixed convection arises from jet impingement cooling of a heated bottom surface of an open cavity in a horizontal channel filled with porous medium through a numerical study.

Stiriba et al. (2010) had analyzed the effects of mixed convective flow over a three-dimensional cavity that lies at the bottom of a horizontal channel through a numerical study, in which was found that the flow becomes stable at moderate Grashof number and exhibit a three-dimensional structure, while for both high Reynolds and Grashof numbers the mixed convection effects came into play.

A finite element analysis was performed on the conjugated effect of joule heating and magneto-hydrodynamic on double-diffusive mixed convection in a horizontal channel with an open cavity (Rahman et al., 2011).

Laminar mixed convective flow over a three-dimensional open cavity with heating from below at constant temperature was numerically simulated using direct numerical simulation and the most hydrodynamic and thermal aspects of the flow were presented by Stiriba et al. (2013). Magneto-hydrodynamic mixed convection in a lid driven cavity along with a heated circular hollow cylinder positioned at the centre of the cavity was studied numerically by Farid et al. (2013). Altemani and Chaves (1988) presented a numerical study of heat transfer inside a semi porous two-dimensional rectangular open cavity for both local and average Nusselt numbers at the heated wall and for the isotherms and streamlines of the fluid flowing inside the open cavity. Chaves et al. (2005) presented a numerical program in finite volumes applied to the transient natural convection heat transfer by double diffusion from a heated cylinder buried in a saturated porous medium. Chaves et al. (2008) presented a work where it was done a numerical analysis of the heat transfer inside a semi porous two-dimensional rectangular open cavity, where forced and natural convection where considered and the bottom and the opposite wall was heated.

This paper presents a continuation of work of Chaves et al. (2008) using the program development in Chaves et al. (2005) where numerical analysis of heat transfer was done inside a semi porous two-dimensional rectangular open cavity. It is constituted by two vertical parallel plates closed at the bottom by an adiabatic surf ace and open at the top, as indicated in Figure 1.

One of the vertical plates is porous and there is a fluid flow forced normal to it in order to cool the other vertical plate. This second plate transfer a uniform heat flux to the cavity. In addition to the forced convection, the analysis considered the influence of natural convection effects. Isotherms and streamlines are presented for the fluid flow inside the open cavity. Local and average Nusselt numbers are obtained for the uniformly heated plate for several values of aspect ratio to the parameters governing the heat transfer: Re_p and Gr.

METHODOLOGY

The conservation equation of mass, momentum and energy, as well as their boundary conditions, will be expressed for the system indicated in Figure 1. Due to the low velocities usually associated with permeable walls, the natural convection will be considered in the analysis. It is assumed that the flow is laminar and occurs under steady state conditions. The natural convection will be treated via the Boussinesq approximation, that is, density variations are accounted for only when they contribute to buoyancy forces. In this problem, the buoyancy term is obtained from the y momentum equation terms representing the pressure and body forces:

$$-\frac{\partial p}{\partial y} - \rho \cdot g \quad (1)$$

The density is related to temperature according to the Boussinesq approximation (Patankar, 1980; Kundu and Cohen, 2008):

$$\rho = \rho_p - \rho_p \cdot \beta \cdot (T - T_p) \quad (2)$$

In Equation (2) T_p indicates the temperature of the fluid inlet at the porous wall and ρ_p the corresponding density. The pressure is now expressed in terms of a modified pressure defined as:

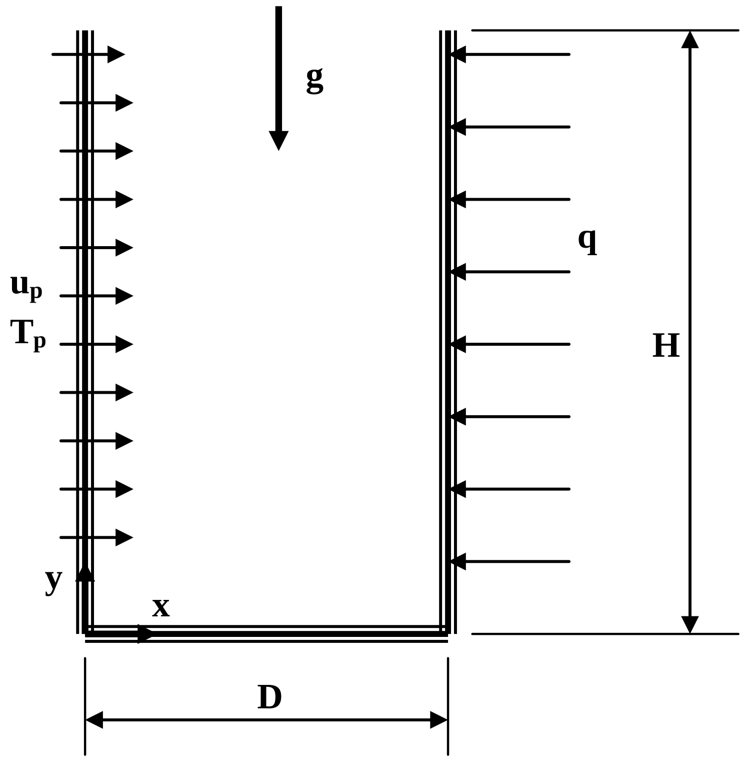

Figure 1. Coordinate system and thermal boundary conditions of the open cavity.

$$p^* = p + \rho_p \cdot g \cdot y \qquad (3)$$

With Equations (2), (3), and (1) can be expressed by:

$$-\frac{\partial p^*}{\partial y} + \rho \cdot g \cdot \beta \cdot (T - T_p) \qquad (4)$$

The second term in this equation relates the buoyancy forces to temperature differences ($T - T_p$). From this formulation, the density will be assumed constant and equals to ρ_p in all the equations, so that the subscript *p* may be deleted. It is also assumed that all the other properties of the fluid are constant. Viscous dissipation and compression work are not considered in the analysis, according to the low velocities, moderate temperature differences and laminar flow conditions assumed. In order to obtain the conservation equations in dimensionless form, the following variables were defined (Patankar, 1980; Kundu and Cohen, 2008):

$$X = \frac{x}{D} \ , \quad Y = \frac{y}{D} \qquad (5a)$$

$$U = u \cdot \frac{D}{\nu} \ , \quad V = v \cdot \frac{D}{\nu} \qquad (5b)$$

$$P = \frac{p^*}{\left(\frac{\rho \cdot \nu^2}{H^2}\right)} \ , \quad \theta = \frac{T - T_p}{\left(\frac{q \cdot D}{k}\right)} \qquad (5c)$$

The equations expressing conservation of mass, x and y momentum and energy then become:

$$\frac{\partial U}{\partial X} + \frac{\partial V}{\partial Y} = 0 \qquad (6)$$

$$U \cdot \frac{\partial U}{\partial X} + V \cdot \frac{\partial U}{\partial Y} = -\frac{\partial P}{\partial X} + \nabla^2 U \qquad (7)$$

$$U \cdot \frac{\partial V}{\partial X} + V \cdot \frac{\partial V}{\partial Y} = -\frac{\partial P}{\partial Y} + \nabla^2 V + Gr \cdot \theta \qquad (8)$$

$$U \cdot \frac{\partial \theta}{\partial X} + V \cdot \frac{\partial \theta}{\partial Y} = \frac{\nabla^2 \theta}{Pr} \qquad (9)$$

In Equations (7) to (9) ∇^2 is the Laplace operator in Cartesian coordinates. These equations are coupled and present two independent parameters, Gr and Pr. The first is the modified

Grashof number, defined by Patankar (1980) and Sharma (2005):

$$Gr = \frac{g \cdot \beta \cdot q \cdot D^4}{k \cdot \nu^2} \quad (10a)$$

and the second is the Prandtl number of the fluid (Patankar, 1980; Sharma, 2005).

$$Pr = \frac{\mu \cdot C_p}{\kappa} = \frac{\nu}{\left(\frac{\kappa}{\rho \cdot C_p}\right)} \quad (10b)$$

At the three solid boundaries of the open cavity, the velocity components are null, except the velocity of injection of the fluid (U_p) at the porous wall. The thermal boundary conditions comprise a uniform (reference) temperature at the porous wall and a specified heat flux at the heated vertical wall. Expressed in dimensionless terms, the boundary conditions become:

$$X = 0\ ;\ U_p = u_p \frac{D}{\nu} = Re_p\ ;\ V = 0\ ,\ \theta = 0 \quad (11a)$$

$$X = 1\ ;\ U = 0\ ;\ V = 0\ ,\ \frac{\partial \theta}{\partial X} = 1 \quad (11b)$$

$$Y = 0\ ;\ U = 0\ ;\ V = 0\ ,\ \frac{\partial \theta}{\partial Y} = 0 \quad (11c)$$

The dimensionless velocity component normal to the permeable wall $\left(u_p \cdot \frac{D}{\nu}\right)$ is one parameter of this problem and it will be denoted the porous wall Reynolds number, Re_p. The outflow boundary of the open cavity, at Y equal to H/D, is just a virtual boundary defining the calculation domain. In order to obtain a solution, two conditions must be satisfied at this boundary. First, there must be no backflow of fluid and second, there must be no diffusion from outside into the calculation domain. The first condition was verified checking the velocity profiles of each result obtained and discarding those results when a backflow was observed. The second was satisfied imposing artificially negligible partial derivatives of θ and U in the vertical direction at the outflow boundary. The velocity component V was corrected at the outflow boundary in order to satisfy the conservation of mass in the whole domain.

The problem presents four independent parameters: H/D, Pr, Re_p and Gr. For a fixed particular fluid, there are still three parameters governing the heat transfer: H/D, Re_p and Gr. In the present work, a single value, equal to 0.72, was assigned to the Prandtl number.

The differential Equations (6) to (9) together with their boundary conditions, Equation (11), comprise a coupled system involving the four variables U, V, P and θ. The equations were discretized using the control volume formulation described in Patankar (1980) and the solution was obtained employing the SIMPLE scheme. The convergence of the results was accepted when the relative change of the dependent variables was under 10^{-3}. From the velocity field solutions, a steam function defined as:

$$\psi = \int_0^Y U \cdot dY \quad (12)$$

was evaluated along lines X = constant, with ψ = 0 at X = Y = O.

From the solution of the temperature field, the local heat transfer coefficient at the heated wall and a corresponding Nusselt number were expressed as Patankar (1980) and Sharma (2005):

$$Nu(Y) = h(Y) \cdot \frac{D}{k}\ ,\ h(Y) = \frac{q}{T_W(Y) - T_p} \quad (13)$$

Where T_W indicates the local temperature of heated wall. With the definition of the dimensionless temperature, Equation (5c), the Nusselt number becomes

$$Nu(Y) = \frac{1}{\theta_w(Y)} \quad (14)$$

An average Nusselt number for the heated wall was obtained from

$$\overline{Nu} = \overline{h} \cdot \frac{D}{k}\ ,\ \overline{h} = \frac{q}{\overline{T}_W - T_p} \quad (15)$$

In Equation (15) $\overline{T}_W$ indicates the average heated wall temperature. Expressed in dimensionless variables, the average Nusselt number becomes.

$$\overline{Nu}(Y) = \frac{1}{\overline{\theta}_w} \quad (16)$$

Where $\overline{\theta}_w$ is evaluated by integrating the dimensionless temperature distribution along the heated wall:

$$\overline{\theta}_W = \frac{D}{H} \int_0^{H/D} \theta_W(Y) \cdot dY \quad (17)$$

The adequacy of the grid fineness employed in the results is presented in Figure 2, related to the average Nusselt number defined in Equation (16). In either the absence or the presence of natural convection effects, a grid of 30x30 was adequate for the aspect ratio of 2 used in most of our results. Increasing the number of grid points from 900 to 1,600 would change the average Nusselt number by 0.2% (Figure 2).

RESULTS AND DISCUSSION

Nusselt number distributions

Initially, just the effects of forced convection on the Nusselt number distributions will be considered to many aspect ratio H/D. The results presented in Figure 3 show that the Nusselt numbers increase with Re_p and that they attain a uniform value within the cavity. The increase of Nusselt number is due to both the larger fluid flow through the cavity and the effect of inertia forces, causing the streamlines to come relatively closer to the heated wall.

The comparison of the streamlines indicated in Figure 4 shows that a larger fraction of fluid flow occurs closer to

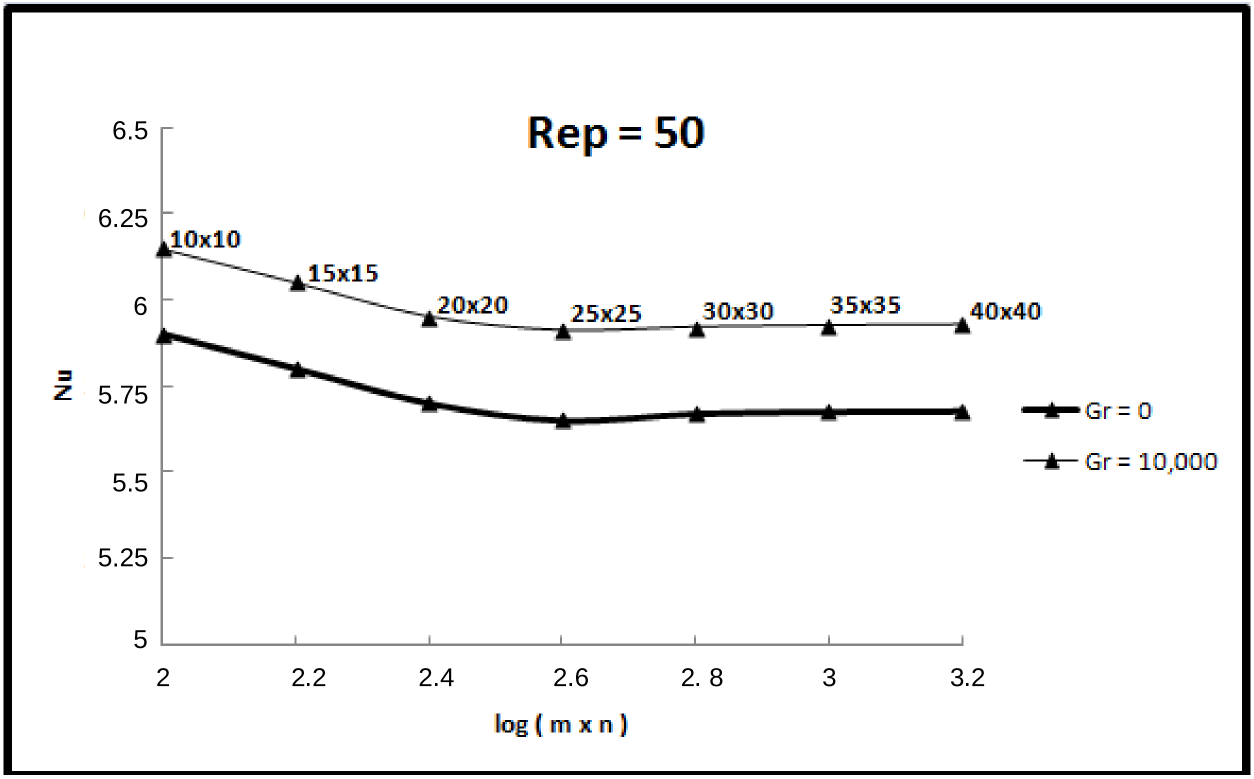

Figure 2. Adequacy of the grid fineness employed.

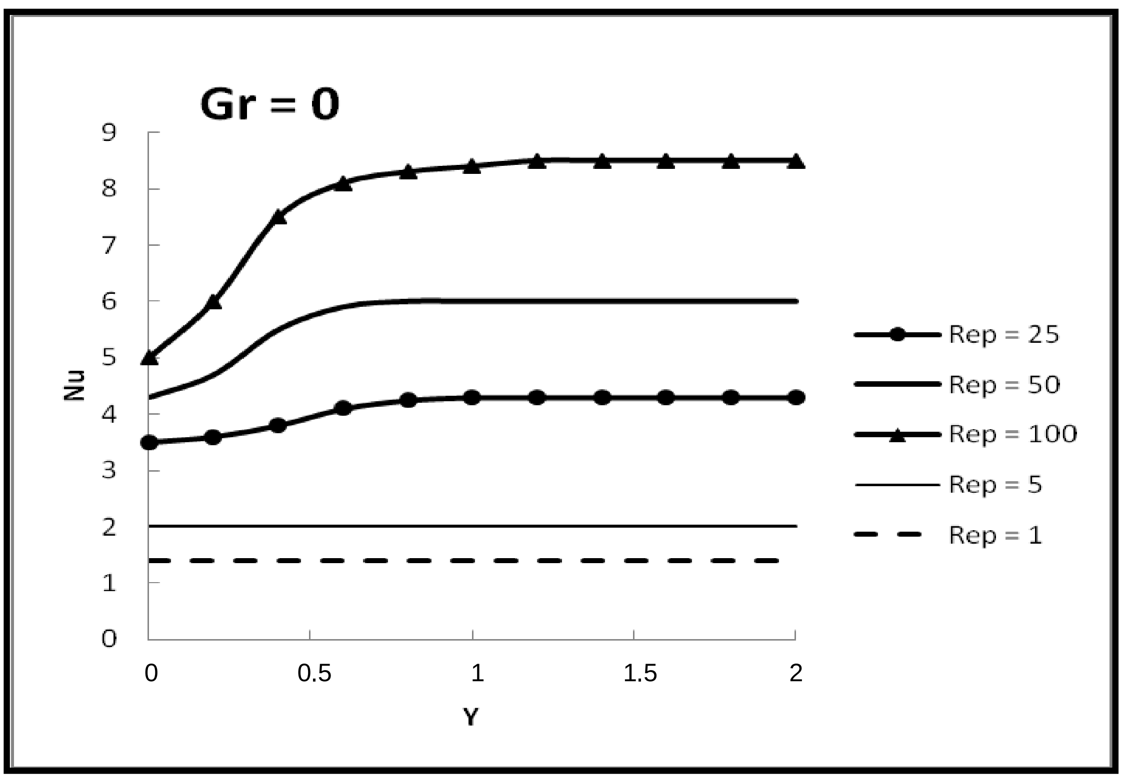

Figure 3. Nusselt number distributions, Gr = 0.

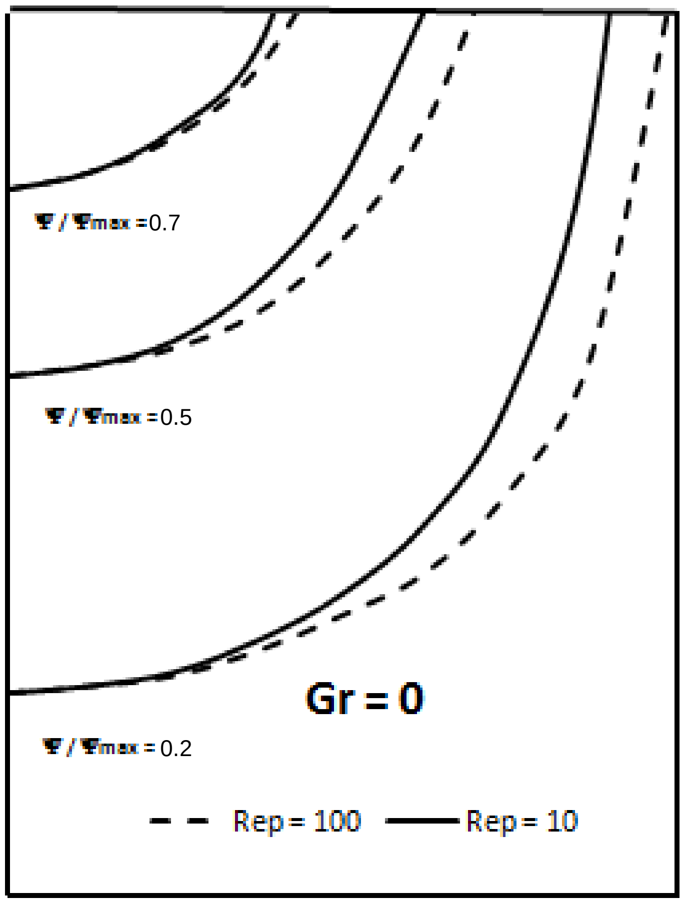

Figure 4. Comparison of streamlines (Ψ/Ψ_{max}) for Gr = 0.

the heated wall when Re increases. In view of the definitions of Nu in Equations (13) and (14), Figure 3 also indicates that h and θ attain uniform values. This thermal behaviour is analogous to that of the two-dimensional stagnation flow (Kays, 1966), mainly when Re_p is small in Figure 3. The increase of fluid flow along the height of the heated wall, due to injection at the permeable wall, causes a smaller thermal penetration into the fluid in the upper portion of the cavity, as indicated in Figure 5. It is evident in Figure 5 the larger thermal resistance near the bottom of the heated wall.

The effects of natural convection on the Nusselt number distributions will now be considered. The results obtained for a relatively low Re_p are show in Figure 6. The curves of Nusselt number distributions are parametrized with the modified Grashof number. For the smallest values of Gr (10 and 100), the distributions are very similar to those shown in Figure 3. In this range of Gr the mechanism of forced convection is still dominant. The isotherms in the fluid are similar to those of Figure 5 and the heated wall thermal resistance is higher near the bottom of the cavity. As the Grashof number increases, there is an enhancement of heat transfer so that, as indicated in Figure 6, the entire heated plate becomes colder. The effects of the buoyancy forces, acting mainly close to the heated wall, share the dominant role on heat transfer with the forced convection effects. The Nusselt number profiles for Gr larger than 10^3 in Figure 6 indicate that the wall temperature initially decreases slightly from the bottom of the cavity and attains downstream a minimum value. The behaviour is distracted by forced convection effects. The minimum wall temperature occurs however, on the lower portion of the cavity instead of on the upper portion, as was the case in Figure 3. Downstream of this minimum, the wall temperature now increases monotonically to the upper end of the cavity. This behaviour is imposed by natural convection effects. The values of the Gr in Figure 6 are limited in the upper range ($Gr < 10^4$) due to the condition of no backflow of fluid at the outflow boundary. In this respect, the effects of natural convection are somewhat restrained for the relatively low value of Re_p in this figure.

The streamlines and isotherms for Re_p = 5 and Gr = 3,000 are showed in Figure 7. Due to the buoyancy induced flow, the streamlines, compared to the case for Gr = 0 in Figure 4, penetrate deeper into the cavity before

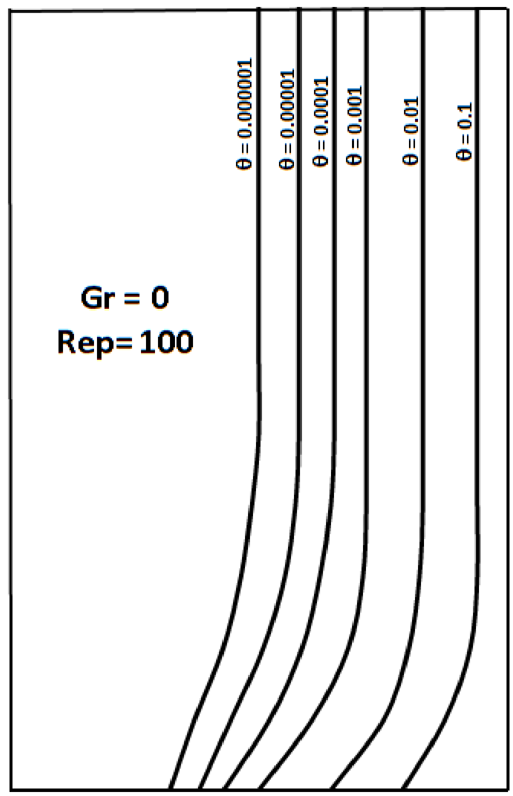

Figure 5. Isotherms for Gr = 0 and Re_p = 100.

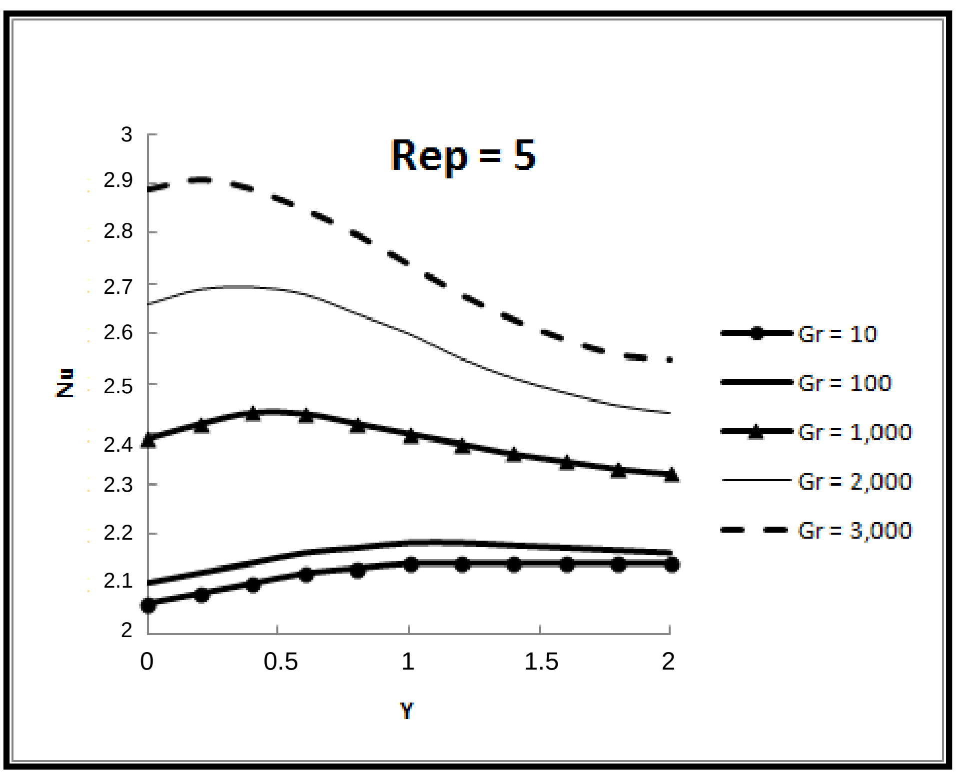

Figure 6. Nusselt number distributions, Re_p = 5.

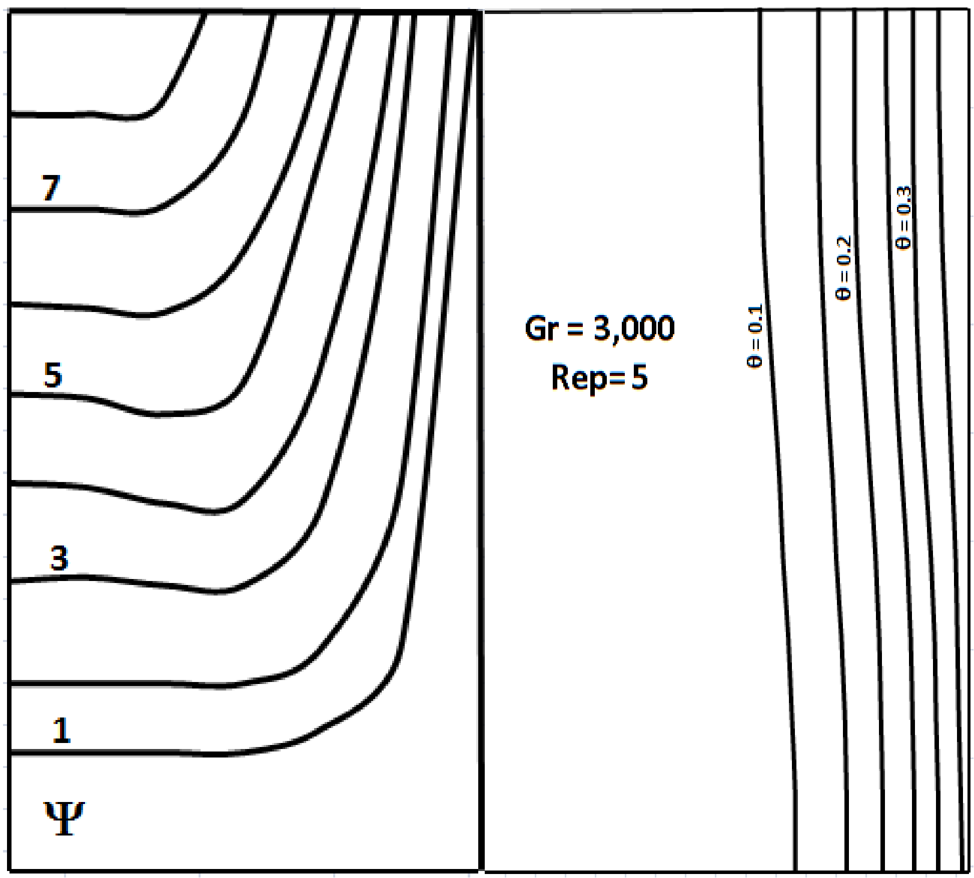

Figure 7. Streamlines and Isotherms for Re_p = 5 and Gr = 3,000.

bending upward. Thus, a large portion of the fluid flow leaves the cavity near the heated wall. The isotherms presented in the same figure give a clear indication of the development of a natural convection boundary layer along the heated wall. It is also noticed an increase of the heated wall thermal resistance very convection effects still predominate.

The Nusselt number distributions for a relatively high Re_p are now shown in Figure 8. Again, for small values of Gr, there is almost no distinction from the case in the absence of natural convection effects. With this Re_p, the parameter Gr can be increased to a much higher value than before without any backflow of fluid at the outflow boundary. For the largest values of Gr in Figure 8, the heated wall temperature is a minimum right at the bottom and increases monotonically along its length. In this case, the natural convection effects control the heat transfer. The streamlines and isotherms shown in Figure 9 correspond to Re_p equal to 30 and Gr = 10^6. The streamlines indicate that now half of the flow leaves the cavity within only 10% of its width, near the heated wall. The streamlines at the bottom go almost straight to the heated wall. The induced buoyant flow causes a bending of these lines slightly downward before turning upward. The isotherms indicate a natural convection boundary layer development form the bottom of the heated wall. There is no increase in the thermal resistance of wall near the bottom of the cavity, as shown by the isotherms closest to the heated wall.

Average Nusselt numbers

The average Nusselt numbers are shown in Figure 10 as function of Re_p and parametrized with the modified Grashof number. The relative enhancement of heat transfer due the effects of natural convection decreases with Re_p. For the largest value of Gr in Figure 10, equals to 10^7, the effects of natural convection are so dominant that the value of Nu is almost independent of Re_p for the range investigated.

Another view is presented in Figure 11, where Nu is shown as a function of Gr and parametrized with respect to Re_p. It is clear that the enhancement of heat transfer by natural convection occurs when Gr attains a minimum value. This Gr seems to increase slightly with Re_p. As noticed before, Nu attains a limit value practically independent of Re_p.

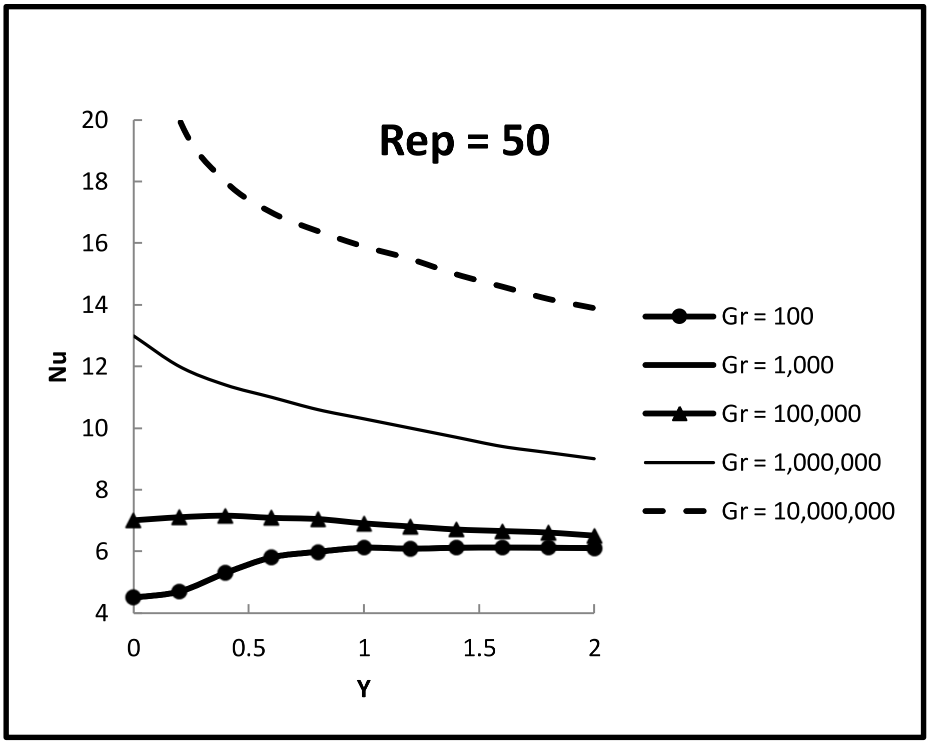

Figure 8. Nusselt number distributions, $Re_p = 50$.

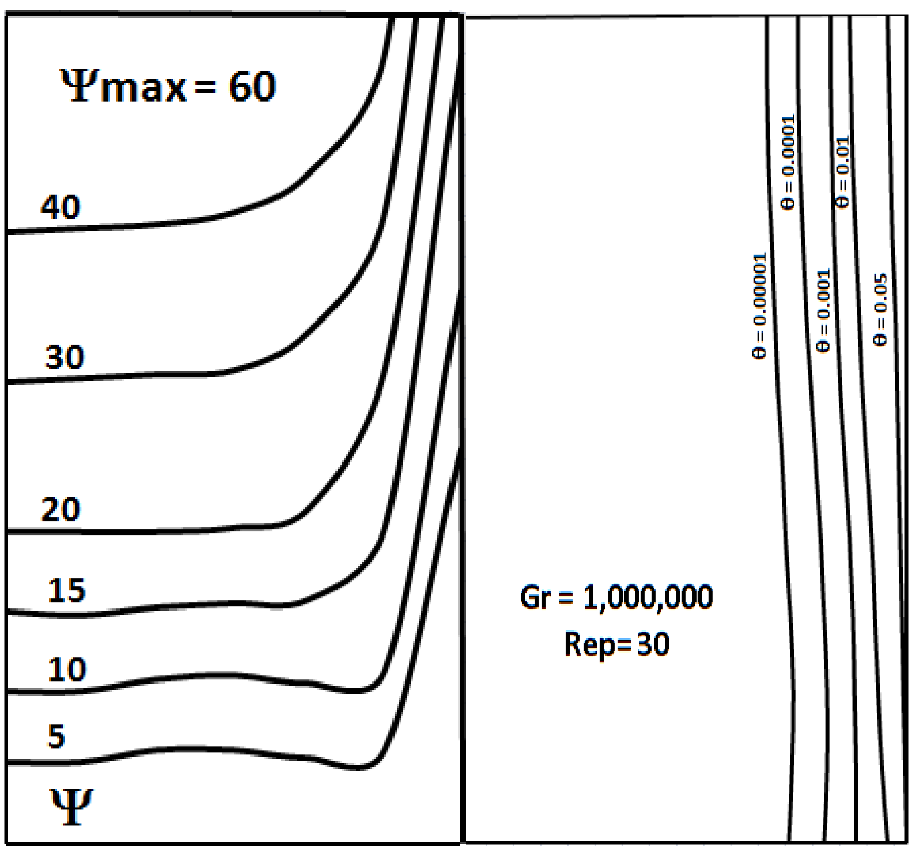

Figure 9. Streamlines and Isotherms for $Re_p = 30$ and $Gr = 10^6$.

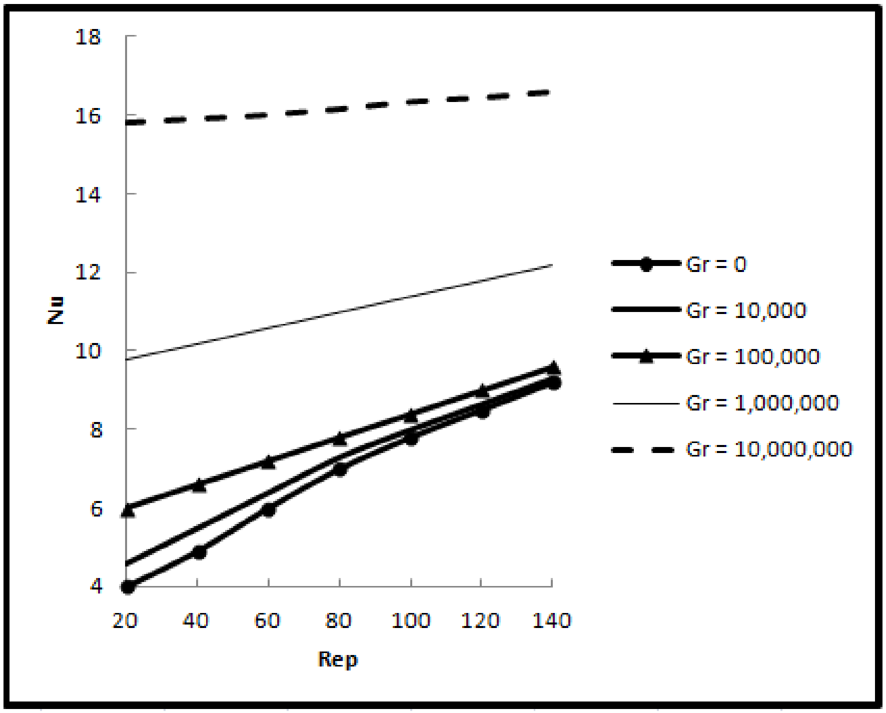

Figure 10. Average Nusselt numbers as a function of Re_p.

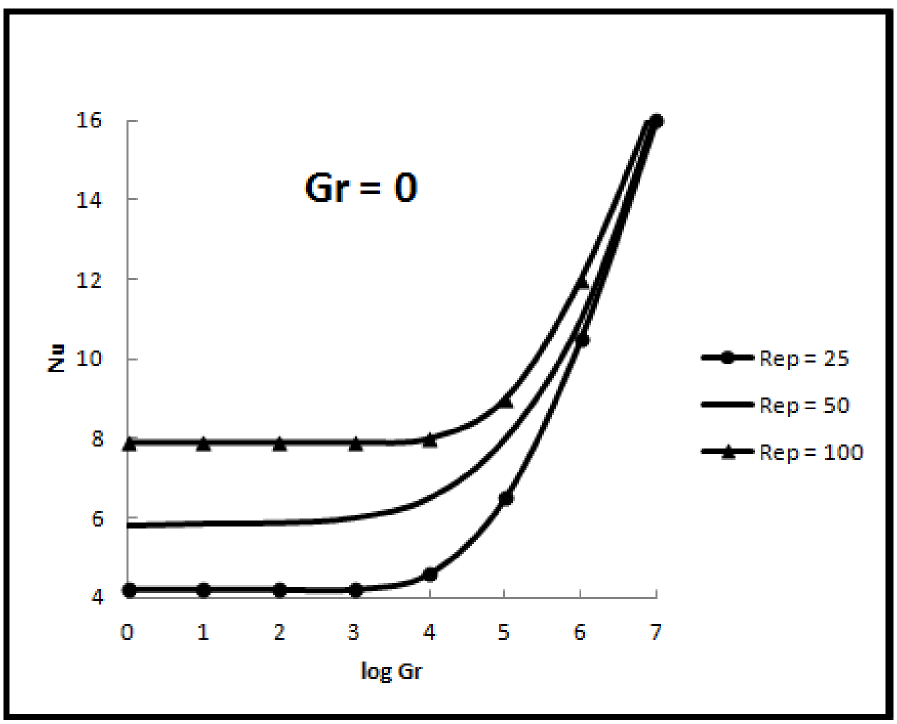

Figure 11. Average Nusselt numbers as a function of Gr.

Aspect ratio

The results presented so far were obtained for an aspect ratio (H/D) of the open cavity equal to 2. In Figure 12, the Nusselt number distributions for the aspect ratios of 2, 4 and 8, obtained for a pair of values of Re_p and Gr, are

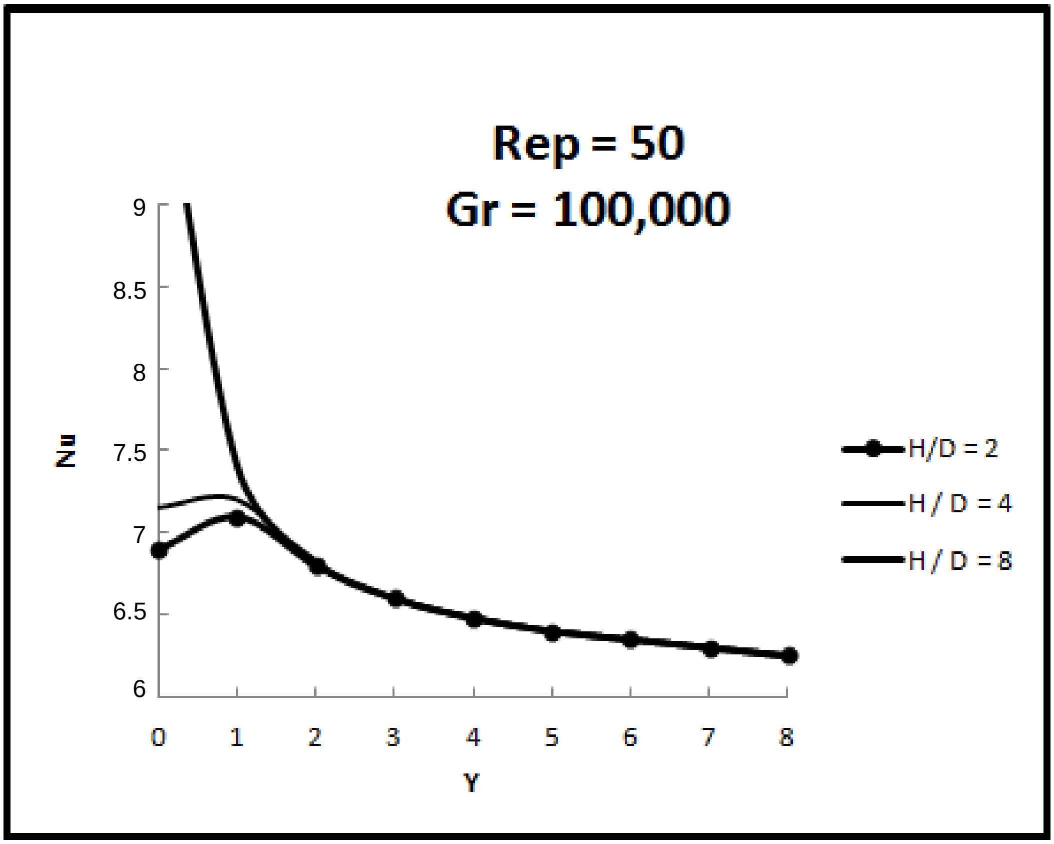

Figure 12. Influence of the aspect ratio.

compared. The distribution for (H/D) equal to 2 is the same as that included in Figure 7, but in a much enlarged vertical scale. As the aspect ratio increases, the minimum temperature of the heated wall moves closer to the bottom of the cavity. As discussed before, this temperature characterizes the start up of a natural convection boundary layer along the heated wall. Thus, these profiles indicate a stronger effect of natural convection as the aspect ratio of the cavity increases. It is also noticed that the Nusselt number distributions in the region controlled by natural convection match each other. In this region the heated wall temperature distributions seem to be independent of the aspect ratio of the cavity.

Conclusions

The study of laminar free and forced convection cooling of a semi permeable open cavity was investigated numerically. The equations describing the problem were expressed in Cartesian coordinates according to stream function formulation and numerically solved by the method of control volume. The program implemented allowed to achieve satisfactory results and enabled a better understanding of the influence of Reynolds and Grashof numbers on flows driven by heat. The results obtained show that the forced convection inside the semi-porous open cavity studied may be greatly enhanced by natural convection effects. When Gr is small enough, just forced convection controls the heat transfer. In this case, the upper portion of the heated plate becomes the most convenient region for cooling purposes. When Gr increases, natural convection effects may become dominant and then the lower portion of the heated plate constitutes the coldest region. When the aspect ratio of the open cavity increases there seems to be an increase of the role played by natural convection effects. The investigation carried out was however, limited because the problem presents four parameters (H/D, Pr, Re_p and Gr) and some choices had to be made about the range to be analysed.

Conflict of Interest

The authors have not declared any conflict of interest.

Nomenclature: C_p, Specific heat at constant pressure [J/kg.^{o}C]; **D,** Width of the open cavity [m]; **g,** Acceleration of gravity [m/s^2]; **Gr,** Modified Grashof number [-]; $\bar{h}$**,** Convective heat transfer coefficient [W/m^2.°C]; **H,** Height of the open cavity [m]; **Nu,** Local Nusselt number [-]; $\overline{Nu}$ **,** Average Nusselt number [-]; **p,** Pressure [Pa]; **p*,** Modified pressure [Pa]; **P,** Dimensionless pressure [Pa]; **Pr,** Prandtl number of the fluid [-]; **q,** Surface heat flux [W/m]; **Re_p,** Porous wall Reynolds number [-]; **T,** Temperature [°C]; **T_p,** Temperature of the porous wall [°C]; **T_w,** Heated wall temperature [°C]; $\bar{T}_w$ **,** Average temperature of the heated wall [°C]; **u_p,** Injection velocity of fluid at the porous wall [m/s]; **U, V,** Dimensionless velocities [m/s]; **x, y,** Cartesian coordinates [m]; **X, Y,** Dimensionless Cartesian coordinates [m]; **β,** Coefficient of thermal expansion [1/°C]; **ψ,** Stream function [-]; **ν,** Kinematic viscosity [m^2/s]; **θ,** Dimensionless temperature [°C]; θ_w**,** Dimensionless heated wall temperature [°C]; $\bar{\theta}_w$**,** Dimensionless average heated wall temperature [°C]; **ρ,** Density [kg/m]; **Σ,** Number of grid points in the domain [-]; **μ,** Viscosity [Pa.s]; **κ,** Thermal conductivity [W/m. °C].

REFERENCES

Altemani CAC, Chaves CA (1988). Convective cooling of a semiporous open cavity. In: XXVI National Heat Transfer Conference, Heat Transfer in Electronics – HTD: ASME, Philadelphia, 111:149-154.

Bairi A, Garcia de Maria JM, Bairi I, Laraqi N, Zarco-Pernia E, Alilat N (2012). 2D transient natural convection in diode cavities containing an electronic equipment with discrete active bands under constant heat flux. Int. J. Heat Mass Transfer 55(19-20):4970-4980.

Bairi A, Laraqi N, Garcia de Maria JM (2007). Numerical and experimental study of natural convection in tilted parallelepipedic cavities for large Rayleigh numbers. Exp. Therm. Fluid Sci. 31(4):309-324.

Bejan A (1984). Convection Heat Transfer. New York, NY: Wiley Interscience,

Boukhanouf R, Haddad A (2010). A CFD analysis of an electronics cooling enclosure for application in telecommunication systems. Appl. Therm. Eng. 30(16):2426-2434.

Bruchberg H, Catton I, Edwards DK (1976). Natural convection in enclosed spaces: a review of applications to solar energy collection. ASME J. Heat Transfer. 98:182-188.

Chan YL, Tien CL (1985). A numerical study of two-dimensional laminar natural convection in shallow open cavities. Int. J. Heat Mass Transfer. 28:603-612.

Chaves CA, Camargo JR, Cardoso S, Macedo AG (2005). Transient natural convection heat transfer by double diffusion from a heated cylinder buried in a saturated porous medium. Int. J. Therm. Sci. 44:720-725.

Chaves CA, Camargo JR, Correa VA (2008). Combined forced and free convection heat transfer in a semiporous open cavity. Sci. Res. Essay. 3(8):333-337.

Farid SK, Billah MM, Rahman MM, Sharif UMd (2013). Numerical study of fluid flow on magneto-hydrodynamic mixed convection in a lid driven cavity having a heated circular hollow cylinder. Procedia Eng. 56:474-479.

Fontana E, Silva A, Mariani VC (2011). Natural convection in a partially open square cavity with internal heat source: An analysis of the opening mass flow. Int. J. Heat Mass Transfer 54(7–8):1369-1386.

Gandhi MS, Ganguli AA, Joshi JB, Vijayan PK (2012). CFD simulation for steam distribution in header and tube assemblies. Chem. Eng. Res. Design 90(4):487-506.

Hess CF, Henze RH (1984). Experimental investigation of natural convection losses from open cavities. ASME J. Heat Transfer 106:33-338.

Juarez JO, Hinojosa JF, Xaman JP, Tello MP (2011). Numerical study of natural convection in an open cavity considering temperature-dependent fluid properties. Int. J. Therm. Sci. 50(11):2184-2197.

Kakaç S, Shah RK, Aung W (1987). Handbook of Single Phase Convective Heat Transfer. New York, NY: John Wiley & Sons,

Kays WM (1966). Convective Heat and Mass Transfer. New York, NY: McGraw-Hill.

Kundu PK, Cohen IM (2008).Fluid Mechanics. 4 ed. New York, NY: Academic Press.

Nickell T (1997). Cooling analysis eliminates fan, reducing weight by 60 % and power draw by 75%. Simulation 68(5):301-303.

Ostrach S (1972). Natural Convection in Enclosures. Adv. Heat Transfer 8:161-227.

Patankar SV (1980). Numerical Heat Transfer and Fluid Flow. New York, NY: McGraw-Hill – Hemisphere.

Penot F (1982). Numerical calculation of two-dimensional natural convection in isothermal open cavities. Numer. Heat Transfer 5:421-437.

Prakash M, Kedare SB, Nayak JK (2012). Numerical study of natural convection loss from open cavities. Int. J. Therm. Sci. 51(1):23-30.

Rahman MM, Saidur R, Rahim NA (2011). Conjugated effect of joule heating and magneto-hydrodynamic on double-diffusive mixed convection in a horizontal channel with an open cavity. Int. J. Heat Mass Transfer 54(15-16):3201-3213.

Shaalan MR, Saleh MA, Mesalhy O, Elsayed ML (2012). Thermo/fluid performance of a shielded heat sink. Int. J. Therm. Sci. In Press, Corrected Proof, Available online 23 June. pp. 1-11.

Sharma PK (2005). Fluctuating thermal and mass diffusion on unsteady free convection flow past a vertical plate in slip-flow regime. Lat. Am. Appl. Res. 35(4):313-319.

Sparrow EM, Stryker PC, Altemani CAC (1985). Heat transfer and pressure drop in flow passages that open along their lateral edges. Int. J. Heat Mass Transfer 28(4):731-740.

Stiriba Y, Ferre JA, Grau FX (2013). Heat transfer and fluid flow characteristics of laminar flow past an open cavity with heating from below. Int. Commun. Heat Mass Transfer 43:8-15.

Stiriba Y, Grau FX, Ferre JA, Vernet A (2010). A numerical study of three-dimensional laminar mixed convection past an open cavity. Int. J. Heat Mass Transfer 53(21-22):4797-4808.

Wong K-C, Saeid NH (2009). Numerical study of mixed convection on jet impingement cooling in an open cavity filled with porous medium. Int. Commun. Heat Mass Transfer 36(2):155-160.

academicJournals

Vol. 10(2), pp. 53-57, 30 January, 2015
DOI: 10.5897/SRE2014.6142
Article Number:1C5D39849789
ISSN 1992-2248

http://www.academicjournals.org/SRE

Scientific Research and Essays

Full Length Research Paper

Safety analysis on hazardous chemicals transportation by Indian roads

Palanisamy Sivaprakash[1]*, Sebastian Joseph[2] and Venkatesan Satheeswaran[2]

[1]Department of Mechanical Engineering, A. S. L. Pauls College of Engineering and Technology, Coimbatore-641032, India.
[2]Department of Mechanical Engineering, Karpagam University, Coimbatore-641021, India.

Received 6 December, 2014; Accepted 12 January, 2015

In engineering industries, necessary safety measures during manufacturing, storage and loading of the chemicals which are dangerous in nature, also known as hazardous chemicals are generally taken. There are means to monitor and control the same, but once the product vehicle is loaded and leaves the plant premises, there is hardly any control over it. The safety of it largely depends on the condition of vehicles and the quality of driver. In this paper, the possible situations creating accidents are discussed and the safety prevention methods are explained.

Key words: Accidents, hazardous chemicals, protection, safety, transportation.

INTRODUCTION

Safety during chemicals transportation is extremely important as it involves the risk of injury or loss to public and/or crew, Environmental pollution, Economic loss and of company image loss, etc. In India, the risk from hazardous chemicals transport is even greater due to ignorance in general, lack of education and training of crew, poor condition of roads and vehicles, lack of amenities to crew and is further compounded due to inadequate concern by the consigner, the consignee, the transport contractor and the transport department authorities. In this study, details of various accidents that had happened due to hazardous chemicals in south India have been studied. Action taken for improving safety in transportation of chemicals, safety rules for transportation of hazardous substances and other relevant legislations in India are mentioned for maintaining safe transportation of hazardous chemicals in the Indian engineering industries. In India the products are mostly transported by road, hence this study is restricted to the transportation of hazardous chemicals by road.

ACCIDENT ANALYSIS

The major types of accidents during the handling of the hazardous substances are process and storage plant accidents, accidents in waste storage area, accident due to transportation and improper handling of hazardous materials during loading or unloading. The eight causes for accidents are mechanical failure, impact, human factors, instrument failure, service failure, violent reaction, external events and upset process conditions. Scientific

*Corresponding author. E-mail: drpsivaprakash@gmail.com

Table 1. Number of Accidents due to hazardous chemicals during the period of April 2011 to March 2012.

Month	Accidents due to solid chemicals	Accidents due to oil usage	Accidents due to gaseous substances
April 2011	7	Nil	Nil
May 2011	7	2	Nil
June 2011	2	Nil	Nil
July 2011	Nil	1	Nil
August 2011	16	1	Nil
September 2011	Nil	Nil	1
October 2011	2	Nil	Nil
November 2011	1	Nil	Nil
December 2011	7	Nil	Nil
January 2012	Nil	6	Nil
February 2012	Nil	Nil	Nil
March 2012	11	Nil	Nil

handling methods of chemicals are always practiced in large industrial units, but the information on such aspects is not readily available and accessible to people working in medium and small scale chemical industries. Unless the workmen know the properties of the chemical and take adequate precaution while handling them, they will be affected by the ill effect of chemicals. So knowledge of hazards to prevent occupational illness is thus of great importance.

Major accidents in South India

Wanda et al. (2004) mentioned in their paper that, 21% of chemical accidents are happening during transportation and the other accident causes involving 39% for equipment failure and 33% for human error. Fabiano et al. (2005) indicated the main areas where the accidents can occur during the road transportation. They are; tunnels bend radii, height gradient, slope, traffic frequency of tank truck, dangerous good truck and other critical areas. Weili et al. (2011) discussed in their paper about the causes and environmental issues of various hazardous chemical accidents in China between 2000 and 2006. During that period most of the accidents had happened by the petroleum and chemical explosives. The details of various accidents that have happened due to hazardous chemicals in south India has been shown in Table 1.

In view of large potential for accidents involving vehicles carrying hazardous chemicals there is lot of scope for improving the quality of vehicles used for transporting chemicals and drivers and also the quality of roads, highways and amenities for the crew members. Chunyang et al. (2004) stated that most of the accidents occur by human error and equipment failure. In the daily life many explosive flammable and toxic substance goods are more dangers hazards when they release improperly. The intimation must be sent to the rescue persons from environmental protection agencies, police and fire departments, poison control centers, hospitals, local media, and other rescue officials immediately in the accident happens.

Safety rules for transportation of hazardous materials

Chee Beng and Chi Bun (1995) explained the safety methods for transport the liquid petroleum gases in the Singapore road ways. In India motor vehicle act is a central act applicable throughout the country. Motor vehicles department in India (http://morth.nic.in/ accessed on 10.08.2013) has prescribed the various Central Motor Vehicle (CMV) rules for hazardous chemical transportation throughout India as mentioned thus.

Safety rules for display labels

CMV rule 137 contains the description of class labels according to the nature of dangerous goods. It further describes the indicative criteria for toxic inflammable chemicals and explosives along with a list of hazardous and toxic chemicals. The CMV rule 129 stipulates the display of distinct mark of the class label to the type of dangerous or hazardous goods as specified in CMV rule 137, and makes it mandatory for every hazardous material carrier to be fitted with appropriate safety devices, including techograph. The CMV rule 129A makes it essential for every hazardous material carrier to be fitted with a spark arrestor as specified by the Bureau of Indian Standards. The CMV rule 130 delineates the manner of display of appropriate class labels on hazardous material carriers. It also specifies the size of letter and placement of class labels on such carrier.

Safety rules for human responsibilities

Jie et al. (2010) noted that, high speeding in the road traffic and the presence of heavily populated residential areas near the road are the dangerous environments may cause the accidents during hazardous chemical transportation. The CMV rule 131 indicated that, the responsibility of the consigner is to have appropriate permit to transport such hazardous goods and to ensure that the owner or transporter and driver one supplied with full and adequate information about the hazardous material being transported and the CMV rule 132 mentioned that, it should be the responsibility of the owner or transporters to ensure that, besides valid registration and permit; the vehicle is safe to transport such hazardous goods and is provided with adequate safety equipments and devices. He should also ensure that the driver being deputed for transportation is trained to handle and transport such hazardous materials and has been provided adequate and correct information, so as to enable him in comply with various safety rules and regulations, as prescribed.

Quarantelli (1991) has mentioned the importance of the emergency response and the problems in planning to the safe transportation of the hazardous chemicals. Tremcard (Transport Emergency Card) is an important document containing details to the driver to transporting hazardous goods in Indian roads. The CMV rule 133 explained that, the major responsibility of the driver is to keep of information provided to him in Tremcard and that to be kept in the drivers cabin also is available at all times while hazardous material related to it is being transported. It is essential for every hazardous material carrier to display correctly the Engineering Information Panel in the format and at places specified under the CMV rule 134, and that it is kept free and clean from obstructions at all times. The owner or transporter of hazardous goods carrier will ensure, to the satisfaction of the consigner that the driver has been provided adequate instructions and training for safe transportation of hazardous material being carried by him as mentioned in CMV rule 135. CMV rule 136 indicates that, it should be the duty of the driver to report to the nearest police station and also to the owner, about the occurrence of accident during transportation of hazardous goods (Figure 1).

Steps to be taken for improving safety in transportation of chemicals

Juan et al. (1995) indicated the seven different classifications of hazardous chemical accidents are; process plant, storage plant, transportation, loading and unloading, waste storage, domestic or commercial and warehouse accidents. Planas et al. (2008) mentioned in their paper about the responsibilities of the owner and driver of the vehicles transporting the hazardous chemicals. As per his statement, the vehicle owner is the one responsible for providing all of the systems for transporting the hazardous chemicals safely. System administrator has to maintain the system properly. The driver is the one to drive the vehicle from the origin to the destination of the goods according to the pre-planned route. The vehicle must carry all of the safety systems like sensors to find out the position of the vehicle. Tremcards in different languages are to be published for all products, by-products and even for the imported raw materials, which are required to be transported by road, similarly, the instructions to drivers and cleaners in different languages are to be published. The appropriate emergency information is displayed on all the vehicles transporting chemicals. Self adhesive stickers are to be kept ready for correcting, if necessary, the emergency information panels on the customer's vehicles when they arrive for loading. A painter should be available to paint the emergency information panels on the customers vehicles is required.

Fitness of vehicle and crew members

In order to ensure the good condition of vehicle and the safety of crew members, the following points need to be checked each time a vehicle reports for loading, which include valid driving licence, condition of the vehicle, fire extinguishers, statutory documents like licence from the inspector of explosives and insurance, instruments and fittings like pressure gauge, rota gauge, temperature indicator and relief valve, protection of fittings against accidental damage, proper emergency information panels, tallying of gross and tare weights painted on the vehicles with the corresponding figures in the permit, availability of appropriate printed instructions to drivers and cleaners and the Tremcard, availability of wheel checks, any source of ignition like lighted agarbatti, cigarette etc., random breath analysis of drivers to check alcohol consumption and availability of tool box, emergency light or battery torch, personal protective equipment, eye-wash bottle and first aid box. Though some regular contractors provide the necessary personal protective equipments like polyvinyl chloride gloves, safety goggles, etc. most of the customers hired vehicles do not have these personal protective equipments. In each case the required personal protective equipments are to be provided at the loading station. For certain products like benzene, the breathing apparatus should also be provided.

Qualification of crew and special training

Kevin et al. (2003) noted in their paper that, many explosive flammables are dangerous when they release improperly and they create great challenge to the environmental pollution. Crew members engaged in transportation of hazardous chemicals must have a certain minimum level of education. Arrangements should

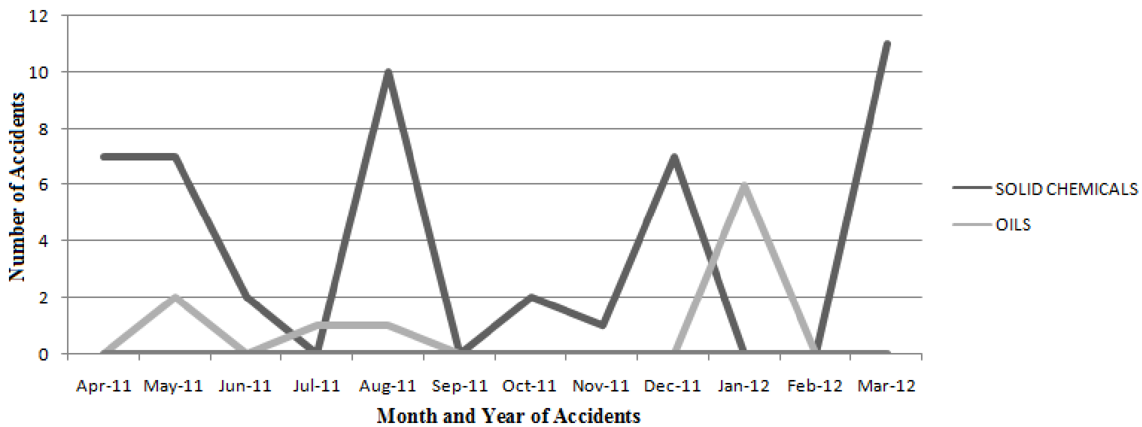

Figure 1. Hazardous chemical accidents level during the period of April 2011 to May 2012.

be made for imparting special training in transportation of hazardous chemicals by road and it should be endorsed in their driving licence or a special licence or certificate should be issued to the trained drivers. Also, the motor vehicles rules should be complied with so as to permit only specially trained drivers, who possess valid special licence or certificates to drive the vehicles carrying hazardous chemicals. These drivers should also be given a periodic refresher course.

The transport contractors should collect the drivers and cleaners who are literate and physically fit. The training programmes are to be conducted for all the product drivers once in every six month, including defensive driving techniques, prescribed routes and prohibited routes, emergency procedures, emergency communication, hazards associated with various chemicals, emergency action code, use of fire extinguishers, loading and unloading procedures, general knowledge of the customers facilities, general inspection of the vehicles, minor repairs of the vehicle, maintaining proper logs, and preparing accident report. Tom et al. (2000) indicated that in common road way the accident can initiate by the major reasons like high volume or road traffic and the presence of populous residential areas. The bypass ways have to be used for chemical transportation by the hazardous chemical transporters.

Safety actions

Ren et al. (2012) mentioned that, hazardous chemical accidents in roads are main issues for public safety. Samuel et al. (2009) also noted the same in their paper and they indicated that, the quick response from the accident area to the rescue personals is very important to solve the problem easily and to reduce human death. For every 3 to 5 km, telephone facility should be made available along all the national highways to enable one to contact the nearest emergency control centre to obtain help promptly or to contact the local police, fire brigade or consigner in the event of an emergency. Prompt penal action should be taken against offending drivers. There should be a deterrent fine for driving without proper licence, driving without lights or with only one headlight at night, using worn out or damaged tyres, overloading or improper loading, carrying passengers on vehicles transporting chemicals and breakdown of vehicles on road because of poor maintenance. Automatic speed monitors (doppler readers) with the television camera, video monitor and recorder should be installed on highways to deter drivers from over-speeding. Also, installation of techograph should be made compulsory on all vehicles carrying hazardous chemicals; this will monitor the driver's performance.

Conclusion

Most of the chemical accidents that happened in south India is because of the careless mistakes and improper handling of materials. The transport contractors are required to check their vehicles thoroughly and issue a 'certificate of fitness' for each vehicle once a month to prevent the accident during hazardous chemical transportation. A sincere joint effort by the industry, the transport contractors and the concerned authorities can surely contribute to bring substantial improvements in all the aspects of road safety and drastically reduce the number of road accidents involving vehicles carrying hazardous chemicals, thereby reducing human suffering and economic loss. Finally, the crew members themselves can contribute a lot by increasing their awareness of the hazards and training.

Conflict of Interest

The authors have not declared any conflict of interest.

REFERENCES

Chee BG, Chi BC, Reginald T (1995). Risk analysis for the road transportation of hazardous chemicals in Singapore – a methodology). J. Loss Prev. Process Ind. 8(1):35-39.

Chunyang W, William J, Rogers M, Sam M (2004). Application of screening tools in the prevention of reactive chemical incidents. J. Loss Prev. Process Ind. 17:261-269.

Fabiano B, Curro F, Reverberi AP, Pastorino R (2005). Dangerous good transportation by road: from risk analysis to emergency planning. J. Loss Prev. Ind. 18:403-413.

Jie Y, Fengying L, Jingbo Z, Ling Z, Lei H, Jun B (2010). A survey on hazardous materials accidents during road transport in China from 2000 to 2008. J. Hazard. Mater.184:647-653.

Juan A, Viichez, SS, Helena M, Joaquim C (1995). Historical analysis of accidents in chemical plants and in the transportation of hazardous materials. J. Loss Prev. Process Ind. 8(2):87-96.

Kevin HD, Zahava B, Gilbert SH, Maureen FO, Wendy EK (2003). Acute public health consequences associated with hazardous substances released during transit, 1993–2000. J. Hazard. Mater. B98:161-175.

Planas E, Pastor E, Presutto F, Tixier J (2008). Results of the MITRA project: Monitoring and intervention for the transportation of dangerous goods. J. Hazard. Mater. 152:516-526.

Quarantelli EL (1991).Disaster planning for transportation accidents involving hazardous materials. J. Hazard. Mater. 27:49-60.

Ren C, Yuan X, Wang J, Zhang X, Li J (2012). Study on emergency response rank mode of flammable and explosive hazardous materials road transportation. Procedia Eng. 45:830 -835.

Samuel C, Keren N, Shelley MC, Steven AF (2009). Frequency analysis of hazardous material transportation incidents as a function of distance from origin to incident location. J. Loss Prev. Process Ind. 22:783-790.

Tom H, Norbert J, John T (2000). Safe handling of combustible powders during transportation, charging, discharging and storage. J. Loss Prev. Process Ind. 13:253-263.

Wanda LW, Rebecca E, Wilburn JK, Ehrlich C, Floridia M (2004). New York hazardous substances emergency events surveillance: learning from hazardous substances releases to improve safety. J. Hazard. Mater. 115:39-49.

Weili D, Guohua C, Qing Y, Qingguang C (2011). The situation of hazardous chemical accidents in China between 2000 and 2006. J. Hazard. Mater. 186:1489-1494.

academicJournals

Vol. 10(2), pp. 58-63, 30 January, 2015
DOI: 10.5897/SRE2014.6110
Article Number:E796F9149791
ISSN 1992-2248

http://www.academicjournals.org/SRE

Scientific Research and Essays

Full Length Research Paper

Growth pattern of two crop species on bio-remediated hydrocarbon polluted soils

Agbor R. B.[1]*, Ekpo I. A.[1], Kalu S. E.[1], Bassey I. U.[2], Okoi E. P.[1] and Ude E. O.[1]

[1]Department of Genetics and Biotechnology, University of Calabar, P. M. B 1115 Calabar, Cross River State, Nigeria.
[2]Department of Microbiology, University of Calabar, P. M. B 1115 Calabar, Cross River State, Nigeria.

Received 7 September 2014; Accepted 12 January, 2015

The effectiveness of agricultural wastes as bioremediation materials is gaining research attention as a better option in mitigating the issue of crude oil effects in soil environment. In the present study, the growth performance of *Telfairia occidentalis* and *Arachis hypogaea linn* in crude oil polluted soil amended with plantain peels (PP) and cocoa pod husks (CPH) were investigated. Eight kilograms (8 kg) each of dried soil samples were collected and weighed into 60 polythene bags. The polythene bags except the pristine control were polluted with 80 ml of crude oil and allowed for 14 days of soil acclimatization. The treatments comprising of CPH and PP were amended after 14 days, using the following concentrations: 0, 100, 150 and 200 g and allowed to acclimatize for 60 days. *T. occidentalis* and *A. hypogaea linn* were cultivated immediately after treatment regimen. The pH of the amended and un-amended soil samples were observed to be at a range recommended for effective bioremediation of hydrocarbon polluted soil. The organic carbon content of the CPH amended soils were significantly reduced as compared to the PP amended soil. The phosphorus, nitrogen, potassium and other essential soil parameters evaluated were significantly high ($P<0.05$) in CPH amended soil than the PP amended soil. Crops grown in the rehabilitated soils possess a high adaptability in CPH amended soil than the PP amended soil. The amendments most preferably cocoa pod husks which tend to be more effective in the reduction of hydrocarbon content of the soil should be utilized in the enhancement of microbial degradation of crude oil product in soils.

Key words: Crude oil, bioremediation, pollution, amendment, cocoa pod husk, plantain, groundnut, fluted pumpkin.

INTRODUCTION

Environmental pollution is a major problem which affects biodiversity, human health, aquatic and terrestrial habitat. The Niger Delta eco-region of Nigeria has been associated with frequent oil spills resulting from oil pipeline vandalization, tanker accidents and accidental rupture of oil pipelines. These mishaps result in the release of crude oil refined petroleum products into terrestrial and aquatic environments. Contamination of soil by crude oil spills is an environmental problem that often requires cleaning up of the contaminated sites

*Corresponding author. E-mail: agborreagan@yahoo.com, reagan2014@unical.edu.ng.

(Bundy et al., 2007). Crude oil spills affect plants adversely by creating conditions which make essential nutrients like nitrogen and oxygen needed for plant growth unavailable to them. Oil pollution in whatever form is toxic to plant and soil microorganisms, pollution studies have described that oil spills kill agricultural plants or inhibit the growth performance of an entire vegetation cover. Plants have been described as the first victim of an oil spill impacted site. Ogbo et al. (2009) reported that oil in the soil creates unsatisfactory conditions for plant growth probably due to non-sufficient aeration of the soil. Oil readily penetrates the pore space of terrestrial vegetation following any spills with heavier friction which may block the pores and this subsequently impedes photosynthesis and other physiological processes in plant (Ogbo et al., 2009). Adam and Duncan (2002) reported that this effect could be due to the oil which acts as a physical barrier preventing or reducing access of seeds to water and oxygen. One of the environmental challenges posed by oil pollution is the alteration in the physical and chemical nature of the soil. Ekpo et al. (2012) reported that plants like cassava, *Thaumacoccus danielli* and sweet potatoes are tolerant to crude oil pollution. While Agbor et al. (2012) reported that the growth performance of some plants in crude oil polluted soil could be ascertained through effective remediation of the soil to reduce the hydrocarbon content of such environment. Biostimulation has been described as an effective method in the remediation of crude oil polluted soil since it involves the use of economically friendly waste (cocoa pod husks and plantain peels) which are not toxic to soil microorganisms but tend to enhance the proliferation of microorganisms in the soil.

Sequel to this, it is pertinent to reduce the hydrocarbon contents of the soil used for agricultural purposes through remediation. In this present study assessment of the growth performance of *Telfairia occidentalis* and *Arachis hypogaea* linn in plantains peels and cocoa pod husks amended soil were evaluated.

MATERIALS AND METHODS

Collection of materials and study site

Mature seeds of *T. occidentalis* and that of *A. hypogaea linn* were purchased from Marian Market Calabar. The plantain peels and cocoa pod husks were collected from Bashua village in Boki Local Government Area, Cross River State while the crude oil (Bonny light) was obtained from the Nigerian Agip Oil Company (NAOC) Port-Harcourt, Rivers State Nigeria. The study was conducted in Step - B Project Site, University of Calabar.

Sample collection and pollution

Top soil (0-25 cm depth) was collected from four points around Biological Science Experimental Farm (BSEF), bulked to form composite soil sample. The soil was air dried and eight kilograms (8 kg) each was weighed into sixty (60) polythene bags. The soil was then polluted with 80 ml of crude oil and kept for fourteen (14) days. This was to allow indigenous microorganisms present in the soil to be acclimatized with the new condition. After fourteen days, the different amendments were applied as shown in Table 1.

Preparation of cocoa pod husks and plantain peels

The collected cocoa pod husks and plantain peels were air dried for thirty (30) days and crushed to powder using electric blender (Diesel engine R175). The powdered materials were stored in containers.

Application of amendment

The CPH and PP were applied to the various polythene bags as shown in the combination Table 1. However, after the treatment, the soil was allowed for sixty (60) days for biodegradation of crude oil in the soil. During this period 200 ml of water was applied to each of the bags every two (2) day to keep the soil environment moist.

Sowing of seeds

After 60 days of remediation, mature seeds of both plants were used for planting. The seeds were sown into the soil in the polythene bags. Sowing was done to assess the growth performance of the remediated soil.

Determination of physico-chemical parameters of soil

Estimation of physico-chemical parameters of the soil was done using the method of Eno et al. (2009). The following parameters were analyzed: Moisture, organic carbon, particle size, nitrogen, phosphorus, potassium, magnesium, sodium, aluminium, hydrogen, pH, exchangeable cation exchange capacity, base saturation and electrical conductivity.

Data collection

Data were obtained on the following parameters: days to seedling emergence, numbers of leaves, leaf length measured using tape, leaf area measured using graph sheet, plants height measured using tap and leaf width measured using tape.

Statistical analysis

Data collected were subjected to a two-way analysis of variance (ANOVA) while significant means were separated using least significant difference (LSD) tests at 5% probability level.

RESULTS

Growth performance of *T. occidentalis* on crude oil remediated soil using cocoa pod husks and plantain peels

The result obtained shows that cocoa pod husks (CPH) at different concentrations significantly increases ($p < 0.05$) the plant height of *T. occidentialis* than plantain peels. The highest plant height between CPH and PP

Table 1. Treatment combinations of cocoa pod husks and plantain peels**.**

Amendment	Plants	Concentrations	Combinations
CPH	TO	PC	CPH TO PC
		COC	CPH TO COC
		100 g	CPH TO 100 g
		150 g	CPH TO 150 g
		200 g	CPH TO 200 g
	AHL	PC	CPH AHL PC
		COC	CPH AHL COC
		100 g	CPH AHL 100 g
		150 g	CPH AHL 150 g
		200 g	CPH AHL 200 g
PP	TO	PC	PP TO PC
		COC	PP TO COC
		100 g	PP P TO 100 g
		150 g	PP P TO 150 g
		200 g	PP TO 200 g
	AHL	PC	PP AHL PC
		COC	PP AHL COC
		100 g	PP AHL 100 g
		150 g	PP AHL 150 g
		200 g	PP AHL 200 g

Twenty treatment combinations were used and replicated thrice to give sixty plots. CPH, Cocoa pod husks; TO, *Telferia occidentalis;* AHL, *Arachis hypogaea linn;* PP, plantain peels; PC, pristine control; COC, crude oil control.

was observed at concentrations of 150CPH and 150PP (Table 3). The number of leaves, leaf width, leaf length and leaf area was also observed to be significantly high in cocoa pod husks (CPH) remediated soil at different concentrations, this was followed by plantain peels (PP) remediated soil. The improvement in the morphological attributes of the *T. occidentalis* was observed to be dose dependent (Table 1). It was observed that prolonged days to germination of *T. occidentalis* was recorded in crude oil control soil followed by pristine control, 100CPH, 150CPH, 2000CPH and 150PP with no significant difference (P > 0.05) in days to germination while 150PP and 200PP had the shortest days to germination (Table 2).

Growth performance of *A. hypogaea linn* on crude oil remediated soils using cocoa pod husks and plantain peels

Bioremediation is a better tool in achieving optimum growth of plant in hydrocarbon polluted environment. It was observed that the amendment of crude oil polluted soil with 150CPH and 200CPH significantly increase (P < 0.05) the plant height of groundnut plant than the control group. The result also shows that 100CPH, 150PP and 200PP had no significant difference (P > 0.05) in the plant height of groundnut but significantly higher (P < 0.05) than the control group. The crude oil control groups had the shortest plant height which implies that the amendments were effective and significantly reduced the hydrocarbon content of the soil as shown in Table 4. The result also shows that 150CPH and 200CPH had significantly higher (P < 0.05) number of leaves than the control group while the control group, 100CPH, 100PP, 150PP and 200PP had no significant difference (P > 0.05) in the number of leaves but significantly higher than the crude oil control groups, thus, indicating the effect of the oil. The leaf width was significantly increased (P < 0.05) in soil amended with 150CPH and 200CPH than the control group while 100CPH, 150PP and 200PP had no significantly difference (P > 0.05) in leaf width but significantly higher (P < 0.05) than the pristine control group. The soil remediated with 100PP and the pristine control showed no significant difference (P > 0.05) in leaf width which were not significantly higher (P < 0.05) than the crude oil control group (Table 3).

However, the leaf length and leaf area in CPH remediated soil were significantly higher (P < 0.05) than that of PP amended soil. Delay in days to germination was observed in crude oil amended soil while the soil amended with high concentrations of the waste

Table 2. Morphological attributes of fluted pumpkin on remediated soils.

Parameters	PC1	COC1	100CPH	150CPH	200CPH	PC2	COC2	100PP	150PP	2000PP	LSD
Plant height	$34.18^b \pm 0.16$	$20.5^e \pm 0.09$	31.3^c 0.10	$34.18^b \pm 0.18$	$40.97^a \pm 0.11$	$10.3^g \pm 0.11$	$11.22^g \pm 0.08$	$16.12^f \pm 0.05$	$22.48^e \pm 0.12$	$27.05^d \pm 0.06$	2.23
No. leaves	$28.00^d \pm 0.08$	$11.83^g \pm 0.06$	$31.33^c \pm 0.10$	$35.33^b \pm 0.14$	$39.83^a \pm 0.16$	$19.00^f \pm 0.08$	$8.00^h \pm 0.07$	$19.83^f \pm 0.06$	$24.83^e \pm 0.09$	$28.33^d \pm 0.10$	2.23
Leaf width	$10.67^c \pm 0.05$	$8.63^d \pm 0.02$	$13.35^b \pm 0.08$	$14.05^b \pm 0.04$	$15.03^a \pm 0.06$	$5.9^f \pm 0.02$	$4.07^g \pm 0.02$	$5.82^f \pm 0.03$	$6.75^f \pm 0.07$	$7.65^e \pm 0.03$	0.79
Leaf length	$10.58^c \pm 0.06$	$6.37^d \pm 0.03$	$13.00^b \pm 0.06$	$14.5^a \pm 0.04$	$14.88^a \pm 0.05$	$6.07^d \pm 0.06$	$4.03^e \pm 0.04$	$7.47^d \pm 0.03$	$7.92^d \pm 0.04$	$8.25_d \pm 0.05$	1.10
Leaf area	$47.5^d \pm 0.24$	$27.67^h \pm 0.15$	$61.17^c \pm 0.03$	$70.33^b \pm 0.09$	$82.17^a \pm 0.18$	$32.5^g \pm 0.24$	$19.33^i \pm 0.20$	$36.00^f \pm 0.17$	$43.00^e \pm 0.16$	$48.67^d \pm 0.10$	3.22
Days for germination	$7.00^c \pm 0.06$	$13.33^a \pm 0.08$	$8.67^c \pm 0.09$	$8.00^c \pm 0.03$	$7.67^c \pm 0.04$	$7.00^c \pm 0.01$	$11.33^b \pm 0.06$	$7.00^c \pm 0.03$	$6.00^d \pm 0.04$	$5.00^e \pm 0.06$	0.78

Means with the same case letter along the horizontal array indicate no significant difference (P > 0.05). PC1: Pristine control, COC: crude oil control.

Table 3. Morphological attributes of groundnut on crude oil remediated soils.

Parameter	PC1	COC1	100CPH	150CPH	200CPH	PC2	COC2	100PP	150PP	200PP	LSD
Plant height	$29.62^d \pm 0.20$	$16.84^e \pm 0.14$	$28.67^c \pm 0.09$	$31.43^b \pm 0.11$	$34.8^a \pm 0.24$	$25.45^d \pm 0.08$	$13.58_e \pm 0.05$	$17.8^d \pm 0.05$	$21.48^c \pm 0.06$	$23.9^c \pm 0.07$	2.46
No. leaves	$15.69^b \pm 0.11$	$6.67^c \pm 0.04$	$18.83^b \pm 0.08$	$26.17^a \pm 0.10$	$27.17^a \pm 0.12$	$13.33^b \pm 0.06$	$6.67^c \pm 0.04$	$17.00^b \pm 0.05$	$19.5^b \pm 0.07$	$22.00^b \pm 0.11$	3.14
Leaf width	$3.5^c \pm 0.09$	$2.33^d \pm 0.02$	$5.2^b \pm 0.03$	$6.62^a \pm 0.01$	$6.88^a \pm 0.04$	$3.33^c \pm 0.01$	$1.8^d \pm 0.01$	$3.33^c \pm 0.02$	$4.58^b \pm 0.01$	$5.22^b \pm 0.04$	0.82
Leaf length	$10.38^b \pm 0.03$	$8.6^c \pm 0.02$	$9.82^b \pm 0.06$	$11.47^a \pm$ o.10	$11.75^a \pm 0.05$	$4.77^d \pm 0.03$	$2.77^d \pm 0.02$	$3.63^d \pm 0.02$	$3.83^d \pm 0.01$	$3.88^d \pm 0.02$	1.00
Leaf area	$27.5^b \pm 0.16$	$29.67^b \pm 0.11$	$2967^b \pm 0.14$	$31.30^b \pm 0.20$	$34.83^a \pm 0.13$	$12.67^d \pm 0.09$	$8.1^e \pm 0.06$	$15.5^d \pm 0.07$	$19.5^c \pm 0.10$	$22.3^c \pm 0.09$	2.83
Days for germination	$6.00^b \pm 0.02$	$8.67^a \pm 0.04$	$5.00^c \pm 0.03$	$4.33^d \pm 0.03$	$4.00^d \pm 0.02$	$5.33^c \pm 0.04$	$9.00^a \pm 0.03$	$6.00^b \pm 0.07$	$4.33^d \pm 0.02$	$4.00^d \pm 0.04$	0.56

Mean with the same alphabet along the horizontal axis represent no significant difference (P > 0.05).

germinated faster than the control groups (Table 3).

Physico-chemical properties of the amended soil using cocoa pod husks and plantain peels

The moisture content of the soil was observed to be high in 200PP amended soil followed by 200CPH, 100PP, and 150PP amended soil. The soil with 100CPH and the crude oil control had no significant difference (P > 0.05) while the pristine control group produces the lowest moisture content. The pH of the amended soil was significantly high (P < 0.05) in all the treated groups with no significant difference (P > 0.05) in pH range. Among the treated soil it was observed that cocoa pod husks and plantain peels at different concentrations significantly reduce (P < 0.05) the organic carbon content of the soil as compared with the crude oil control soil while the pristine control had the lowest organic carbon content (Table 4). The phosphorus contents of the soil was observed to be significantly high (P < 0.05) in 200CPH amended soil and pristine control groups. However, the different amendments significantly increase (P < 0.05) the phosphorus content of the soil as compared with the crude oil control groups that had the lowest phosphorus content. The result also shows that there were no significant difference (P > 0.05) in the magnesium, potassium, H^+, Al^{3+}, sodium, ECEC and H of the soil (Table 4).

DISCUSSION

Physico-chemical properties of crude oil amended soil using cocoa pod husks and plantain peels

The physical and chemical properties of the soil determine to a large extend the microbial activity of the soil and also the performance of plant. Over the past few decades in oil producing communities,

Table 4. Physico-chemical properties of the soil amended with cocoa pod husks and plantain peels.

Parameters	PC1	COC1	100CPH	150CPH	200CPH	PC_2	COC_2	100PP	150PP	200PP	LSD
Moisture	14.5 ± 0.12	16.8 ± 0.09	16.9 ± 0.05	15.8 ± 0.07	22.6 ± 0.04	14.5 ± 0.12	16.8± 0.09	19.6± 0.05	20.3± 0.06	23.4± 0.08	0.72
pH	5.6 ± 0.03	5.9 ± 0.04	7.2 ± 0.02	7.6 ± 0.03	7.8 ± 0.02	5.6±0.01	5.9 ± 0.04	7.0 ± 0.03	7.2 ± 0.03	7.4 ± 0.04	0.92
Org. c.	1.10 ± 0.02	4.86 ± 0.01	2.7 ± 0.01	2.5 ± 0.02	2.30 ± 0.01	1.10± 0.03	4.86 ±0.01	3.0 ± 0.02	3.0 ± 0.01	2.8 ± 0.01	0.69
Nitrogen (%)	0.18 ± 0.01	0.06 ± 0.01	0.19 ± 0.01	0.25 ± 0.01	0.26 ± 0.01	1.10 ± 0.02	0.06 ± 0.01	0.17 ± 0.01	0.20 ± 0.01	0.22± 0.01	0.05
Phosphorus	0.11±0.01	5.83 ± 0.03	40.0 ± 0.08	42.9 ± 0.12	58.2 ± 0.07	0.18 ± 0.01	5.83 ± 0.03	29.9 ± 0.1	36.6 ± 0.04	45.2± 0.13	1.68
Potassium	0.40 ± 0.01	0.16 ± 0.01	0.13 ± 0.01	0.14 ± 0.01	0.18 ± 0.01	43.8 ± 0.11	0.16 ± 0.01	0.11±0.01	0.14± 0.01	0.16± 0.01	0.67
Magnesium	0.98 ± 0.01	0.84 ± 0.01	2.4 ± 0.02	2.4 ± 0.01	2.8 ± 0.01	0.40 ± 0.01	0.84 ± 0.01	1.2 ±0.01	1.2 ± 0.01	1.5 ± 0.01	0.96
Calcium	1.30 ± 0.02	1.20 ± 0.01	9.6 ± 0.04	11.3 ± 0.03	14.6 ± 0.04	0.98 ± 0.01	1.20 ± 0.01	4.9 ± 0.01	6.4 ± 0.03	8.6 ± 0.03	0.65
H^+	1.09 ± 0.01	1.00 ± 0.01	ND	ND	ND	1.30 ± 0.02	1.00 ± 0.01	ND	ND	ND	NS
Al^{3+}	1.00 ± 0.01	0.78 ± 0.01	ND	ND	ND	1.09 ± 0.01	0.78 ± 0.01	ND	ND	ND	NS
Sodium	0.10 ± 0.01	0.14 ± 0.01	0.09 ± 0.01	0.12 ± 0.01	0.14 ± 0.01	1.00 ± 0.01	0.14 ± 0.01	0.06 ± 0.01	0.09 ± 0.01	0.11± 0.01	NS
Exchangeable CEC	2.78 ± 0.03	2.34 ± 0.02	12.2 ± 0.06	13.96 ± 0.1	17.72 ± 0.1	2.78 ± 0.03	2.34 ± 0.02	6.27 ± 0.03	7.83 ± 0.02	10.37± 0.03	7.31
EC	0.56 ± 0.01	0.30±0.01	0.89 ± 0.01	1.10 ± 0.01	1.20 ± 0.01	0.56 ± 0.01	0.30 ± 0.01	0.45 ± 0.01	0.98 ± 0.01	1.0 ± 0.01	0.42
BS	24.82 ± 0.1	23.93 ± 0.2	100 ± 0.00	100. ± 0.00	100.0.00	24.82 ± 0.2	23.93 ± 0.2	100 ± 0.1	100.0.0	100 ± 0.0	7.93

Means with the same case letter along the horizontal array represent no significant difference (P > 0.05).

farm land deterioration and abandonment have been observed due to oil spills on land. Biostimulation potentials of agro-wastes is beginning to gain research attention as better alternative in enhancing microbial degradation of hydrocarbon in soil and possibly improving the physicochemical properties of the soil. Interestingly, the application of cocoa pod husks and plantain peels in crude oil contaminated soil significantly improved the physicochemical properties of the soil. The extent of degradation of hydrocarbon was significantly high in soil amended with cocoa pod husks and plantain peels. The pH level of soil amended with cocoa pod husks was significantly higher than soil amended with plantain peels. However, the pH level of both amended soil was observed to be alkaline. This implies that the amendments have strong buffering capacity in the soil. The result of Agbor et al. (2013) reported that both cocoa pod husks and plantain peels possess strong buffering effect in the soil. Olabisi et al. (2009) also reported that melon shells have strong buffering effect on soil and observed that melon shells helps in enhancing the microbial degradation of the soil. pH range of a particular soil gives an estimate of the nutritional properties as well as the fertility of the soil. It was observed from the result obtained that the pH of the crude oil control (COC) was acidic. The presence of high amount of acidity in soil, could adversely affect soil conditions including microbial activities in the soil. It has also been observed that increased hydrocarbon concentration in the soil reduces the phosphorus and nitrogen content of the soil as observed in the crude oil control. However, Ekpo et al. (2013) reported that the presence of high concentration of crude oil in soil reduces microbial activity in such environment. Offor and Akomaye (2006) had also reported that the availability of nitrogen and phosphorous in hydrocarbon polluted soil stimulate microbial population in the impacted site. The organic carbon content of the soil amended with cocoa pod husks was observed to significantly reduce ($P < 0.05$) than the plantain peels amended soil. The productivity of plant in soil with high organic carbon content could adversely be affected.

Assessment of growth performance of *T. occidentalis* and *A. hypogaea linn* on crude oil remediated soil

The improvement in the growth performance of *T. occidentalis* and *A. hypogaea linn* in the biostimulated soil was higher than the pristine soil and crude oil control soil. This could be attributed to the increase in soil nutrient. It was observed that the higher the concentration of the amendment, the greater the growth performance of the plant. Stewart et al. (1974) observed that increased in nitrogen in soil increases vegetative growth of cassava. The significant reduction in growth performance of *T. occidentalis* and *A. hypogaea linn* in the control soil conformed with the report of Venosa et al. (2002) that crude oil polluted soil reduces the growth of plants. Black (1957) maintained that growth and development of plants are adversely affected by crude oil pollution, ranging from wilting, chlorosis, tissue and cell maceration, blotching and the collapses of marginal necrotic spots, which have eventually resulted in the death of plants. The potentials of these agro-wastes in improving the growth performances of these plants in hydrocarbon polluted environment justified "the result of the physicochemical properties of the soil. That indicates the increase in nitrogen and phosphorus content of the soil. In comparison, among the two agro-wastes cocoa pod husks tend to significantly improve the plant height, leaf area, number of leaves, leaf length and width of the *T. occidentalis* and *A. hypogaea linn* than the plantain peels amended soil. However, this result could also imply that the degradation rate of hydrocarbons in the soil amended with cocoa pod husks are good bioremediation agents.

Conclusion

Therefore, this study had revealed that introduction of crude oil into agricultural soil adversely and severely inhibits plant growth and development as observed in the crude oil control. Thus the soil amended with cocoa pod husks and plantain peels tend to reduce the hydrocarbon content of the soil, and significantly improved the growth of *T. occidentalis* and *A. hypogaea linn* in the soil. It can be concluded that cocoa pod husks and plantain peels are good remediating materials that should be used in the cleaning up of crude oil polluted environment.

Conflict of Interest

The authors have not declared any conflict of interest.

REFERENCES

Adam GI, Duncan H (2002). Influence of Dye on Seed Germination. Environ. Pollution120:363-370.

Agbor RB, Ekpo IA, Udofia U, Okpako U, Ekanem BE (2012). Potentials of cocoa pod husks and plantain peels in the degradation of total petroleum hydrocarbon content of crude oil polluted soil. Archives Appl. Sci. Res. 4(3):1372-1375.

Agbor RB, Ekpo IA, Okpako EC, Osuagwu AN, Ekanem BE (2013). Absorption and Biodegradation of hydrocarbon polluted aquatic environment using Agro-wastes. Int. J. Appl. Res. Technol. 2(1):186-193.

Black CA (1957). Soil Plant Relationship. John Wiley and Sons. Inc. New York. 90:245-290.

Bundy JG, Paton GL, Campbell CD (2007). Microbial Communities in Different Soil Types do not cover after Diesel Contamination. J. Appl. Microbiol. 92:276-288.

Ekpo IA, Agbor RB, Okpako EC, Ekanem BE, Otu PA (2012). Effect of crude oil and stimulated acid rain on the growth and physiology of *Thaumatococcus daniellii.* J. Biodivers. Environ. Sci. 2(9):21-25.

Ekpo IA, Osuagwu AN, Okpako EC, Agbor RB, Ekanem BE (2013). Physicochemical and morphological features of *Talinum triangulare* (water-leaf) exposed to hydrocarbon polluted soil. Global J. Biodivers. Sci. Manag. 3(1):52-57.

Eno JU, Trenchard OI, Joseph AO, Anthony OA, Ivara EE (2009). Manuel of Soil, Plant and Water Analyses. Sibon Books Ltd, Lagos. pp.1-102.

Offor US, Akomaye LA (2006). Amendment of crude oil contaminated soil with sawdust and chromolaena leaves for optimum plant protection. Afr. J. Biotechnol. 5(9):770-774.

Ogbo EM, Zibigha M, Odogu G (2009).Effect of crude oil on growth of the weed (*Paspalum Scrobiculatum* L.) Phytoremediation potential of the plant. Afr. J. Environ. Sci. Technol. 3(9):229-233.

Olabisi PA, Olabimpe AA, Udeme JJI (2009). Biodegradation of crude oil in soil amended with melon shell. Aus. J. Technol. 18(1):34-38.

Stewart BA, Woolhiser DA, Wischmeier WH, Caro JH, Freere MH (1974). Control of water pollution from cropland. Vol. 1, Report EPA-600 US Environmental Protection Agency, Washington DC, USA.

Venosa AD, Lee K, Suidan MT, Garcia –Blanco S, Cobanli S, Moteleb M, Haines TR, Tremblay G, Hazelwood M (2002). Bioremediation and biorestoration of crude oil contaminated freshwater wetland on the St. Lawrence River. Bioremediat. J. 6(3):261-281.

academicJournals

Vol. 10(2), pp. 64-70, 30 January, 2015
DOI: 10.5897/SRE2014.6035
Article Number:7C7AE2449793
ISSN 1992-2248

http://www.academicjournals.org/SRE

Scientific Research and Essays

Full Length Research Paper

Trade, population study and conservation aspects of Choraka/Choru in Kumaun Himalayas

D. Arya[1], D. Bhatt[1], G. C. Joshi[1] and L. M. Tewari[2]

[1]Regional Research Institute of Himalayan Flora, CCRAS, Tarikhet, Ranikhet, Dist Almora-. 263663 Uttarakhand, India.
[2]DSB Campus, Kumaun University, Nainital, Uttarakhand 263002, India.

Received 10 July, 2014 ; Accepted 12 January, 2015

Medicinal plants constitute an effective source of traditional and modern medicine. *Angelica glauca* Edgew. is a high value medicinal aromatic plant species of the Himalaya. In this article, a brief profile of the herbal medicinal plant Choraka (*A. glauca* Edgew.) which is used in the traditional system of medicine and in folk medicines in the Kumaun Himalayas was presented. Regular supply of raw material for pharmaceuticals and ethno-medicinal uses has high pressure on demand to fulfill the demand of the raw material. Adulteration and substitution are common in raw material in trade.

Key words: *Angelica glauca* Edgew, Kumaun Himalaya, adulteration/substitution, trade, population study and conservation.

INTRODUCTION

The Himalaya is rich in biodiversity due to the variety of habitats available in it. Out of the total number of endemics reported for India, about 46% are found in the Indian Himalaya. About 3471 endemic species of flowering plants are reported in the Himalaya. *Angelica* is a genus of aromatic herb, including about 70 species distributed in the North temperate regions. Two species occurs in India: *Angelica archangelica* Linn. and *Angelica glauca* Edgew (Choraka). *Angelica* (Riv.) Linn (umbellifer.) Ind.Kew. *A. glauca*, Edgew in Trans. Linn.soc.xx(1846)53-Reg Himal. Latin name *Angelica* means virtues in medicine and *glauca* means blue, grey green. *A. glauca* Edgew. (Choraka, Gandhrayan) belonging to the family Apiaceae is endemic to the Himalaya, distributed along 2600 to 3700 m a.s.l in Uttrarakhand (Kumaon and Garhwal regions) and is an endangered medicinal herb. Depending upon the distribution and local or commercial use in the Uttarakhand, *A. glauca* is with spare population in few areas and in high demand of restricted distribution heavy pressure (RDPH) (Rawat, 2005). It is found between 2600 to 3700 m asl in western Himalayas. In Uttarakhand the distribution of this plant was mentioned in the valley of flower, Kedarnath, Khatting, Gidara, Kiarki, Changsil, Laspa, Milam (Rawat, 2005). Choraka is a controversial drug with aromatic roots and possess diaphoretic and diuretic properties and are used as spice and condiments by indigenous communities. The roots are considered to be a good cordial and stimulant, used in flatulence dyspepsia and are also useful in constipation. Locally, root powder with milk is given in bronchitis as well as in constipation. Whole herb is reported to be useful to cure stomach troubles, bilious complaints, menorrhagia, infantile atrophy and as a stimulant (Chopra et al., 1956;

*Corresponding author. Email: deepshikhaarya2008@rediffmail.com.

Anonymous, 1948, Shah.et.al. 1970; Anonymous, 1982, Anonymous, 1985; Bisht et al., 2008; Sarin, 2008). Market demand of these species for pharmaceuticals and ethno–medicine utility, are met through harvesting from wild populations. Due to unsustainable harvesting, habit loss and grazing pressure these species have been assigned as endangered for the Himalayan region (Arya et al., 2013; Bhatt et al., 2014a, b; Ved et al., 2003).

Study area

Intensive survey was carried out for the study of *A. glauca* Edgew. From Munsyari to Milam glacier located between 2300 to 4100 m asl Pithoragarh district of Uttarakhand Himalaya during flowering season (July to September). Difference in altitudinal range and climatic condition provide a diverse flora and fauna. Survey of Tanakpur and Pithoragarh was carried out to collect the market information and samples from different traders and dealers for identification of the genuineness of the raw material.

METHODOLOGY

During the market survey, local traders and dealers were identified and interviewed. The raw drug samples of *Choru* were collected to identify the substitute and adulterant. During the flowering season of *A. glauca,* various habitat were identified on the basis of altitude, topography and climatic conditions etc. The plant species was sampled by laying quadrates of 1 m × 1 m size randomly in nine different sites. Milam (moraine), Milam (fellow fields), Martoli, Laspa, Phurkia (Pasture), Phurkia (Scrub), Dwali, Simdim, Tejam. Individuals of all the species were counted in each quadrat. Analytical feature such as density, frequency, relative density were calculated following Mishra (1968). In each site, 30 quadrants were laid randomly. In each quadrat the numbers of individual species were counted as area of occurrence and for the demographic observation of threat category assessment. To determine status of the mean values of each quantitative parameter, three stands of transect were considered for further interpretation. The threat category of a species was identified using six attributes (that is, habitat, preference, distribution range, population size, extraction trend, native and endemic species) and following Samant et al. (1998) and Ved et al. (2003).

RESULTS AND DISCUSSION

Market analysis

During the market survey different traders were identified and interviewed. On the basis of information gathered by interviewing the traders it is found that *A. glauca* is were sold under the main trade names; Gandrayan, Choraka, Choru and is collected from Pithoragarh district in Kumaon region from wild source and cultivators. As leading to a gradual loss in regeneration potential and diversity of economically valuable species, *A. glauca* has been categorized as Globally (IUCN) and in Uttarakhand as Endangered species. Because of the species with sparse population in areas and in high demand (RDHP), there is a gap in supply and demand which leads to substitute and adulterant of the species which may be an addition of low grade or spoiled drug with genuine one. The adulterant is usually a material which is both cheap and available in fairly large amount. Choraka roots are sold at Rs 900 per kg in the market (Table 1, Figures 1 and 2).

Choraka, its substitute and adulterant

In India, two different species viz. *A. glauca* and *A. archangelica* Linn. go under the same vernacular name Choraka. Root and rootstock of both pieces are indiscriminately sold in the market as *A. archangelica* is also an endangered species. *Pleurospermum angelicoides* Benth. is also largely used as a substitute of *A. glauca* in Uttarakhand crude drug market (Arya et al., 2012).

The root of *A. glauca* Edgew. is considered the true source of Gandrayan/Choraka in Ayurvedic text. *A. glauca* rootstock is yellowish to brownish in color (Figure 3). The odour is characteristically aromatic; fracture is hard and fibrous, root is 2.5 mm thick while for *A. archangelica,* the root stock is dark grey brown to reddish and purplish brown in color, 5.0 to 10.0 cm thick, fractures is short and smooth (Figure 4). *P. angelicoides* root is dark brown in color, long conic and aromatic (Figure 6).

Population study

Angelica was found distributed within the different habitat (steep rocky slopes, moist rocky area) in study area (Figure 5). The performance of the species at different sites is presented in Table 2.

The surveyed plant species was scarily distributed in dry open slopes and sometimes on scree slopes (very high altitude glacial moraines and landslide areas). The low frequency, density, relative density shows the poor availability of the species in particular habitat. During the study in all 9 sites it was observed that the maximum frequency (80%) of the plant was observed in Milam (Moraine) and minimum (40%) at Dwali, maximum density at 1.00 plants/m^2 at Phurkia (Scrub) and 0.70 plants/m^2 at Martoli, TBC value ranges between 0.51 to 0.72 cm^2 showing highest value at Laspa and lowest at Milam (Fellow field), IVI pattern of *A. glauca* has highest (10.88) at Milam (Moraine) and lowest (6.76) at Tejam (Figure 7).

Conservation

A. glauca is endemic to the Himalaya; it is an endangered

Table 1. Rates of *Angelica glauca* Edgew. in different markets.

Traded drug	Botanical name	Part used	Market	Years		
				2009 (in kg)	2010 (in kg)	2011 (in kg)
Choraka	*Angelica glauca* Edgew	Root	Tanakpur	825/-	900/-	950/-
			Pithoragarh	800/-	850/-	900/-

Table 2. Performance detail of *A.glauca* Edgew.

Sites	Frequency	Rfr	Abundance	Density	Relative density	TBC	R.dom	IVI
Milam (Moraine)	80.00±3.33	5.05± 0.23	1.13± 0.09	0.90± 0.11	2.36± 0.56	0.67± 0.23	3.47± 0.13	10.88± 0.21
Milam (fellow fields)	56.67± 1.21	3.71± 1.22	1.53± 0.20	0.87± 0.13	2.04± 0.38	0.51± 0.06	3.42± 0.09	9.17± 0.06
Martoli	63.33± 0.55	3.94± 1.12	1.11± 0.07	0.70± 0.11	1.73± 0.51	0.65± 0.011	3.38± 0.23	9.05± 0.13
Laspa	60.00± 2.00	3.77± 0.20	1.28± 0.08	0.77± 0.13	1.54± 0.52	0.72± 0.08	3.94± 0.06	9.11± 0.13
Phurkia (Pasture)	53.33± 1.29	3.74± 0.79	1.69± 0.15	0.97± 0.11	2.10± 0.33	0.67± 0.07	2.798± 0.18	8.63± 0.06
Phurkia (scrub)	60.00±2.31	3.72± 0.86	1.67± 0.20	1.00± 0.15	2.35± 0.99	0.60± 0.07	3.47± 0.27	9.50± 0.17
Dwali	40.00± 2.02	2.65± 0.46	2.08± 0.15	0.83± 0.16	1.88± 0.11	0.65± 0.21	3.47± 0.16	8.00± 0.26
Simdum	70.00± 1.28	4.16± 0.42	1.14± 0.10	0.80± 0.18	1.80± 0.25	0.40± 0.10	2.50± 0.10	8.46± 0.05
Tejam	43.33± 1.45	2.64± 0.75	2.00± 0.13	0.87± 0.12	1.87± 0.33	0.36± 0.10	2.25± 0.10	6.76± 0.29

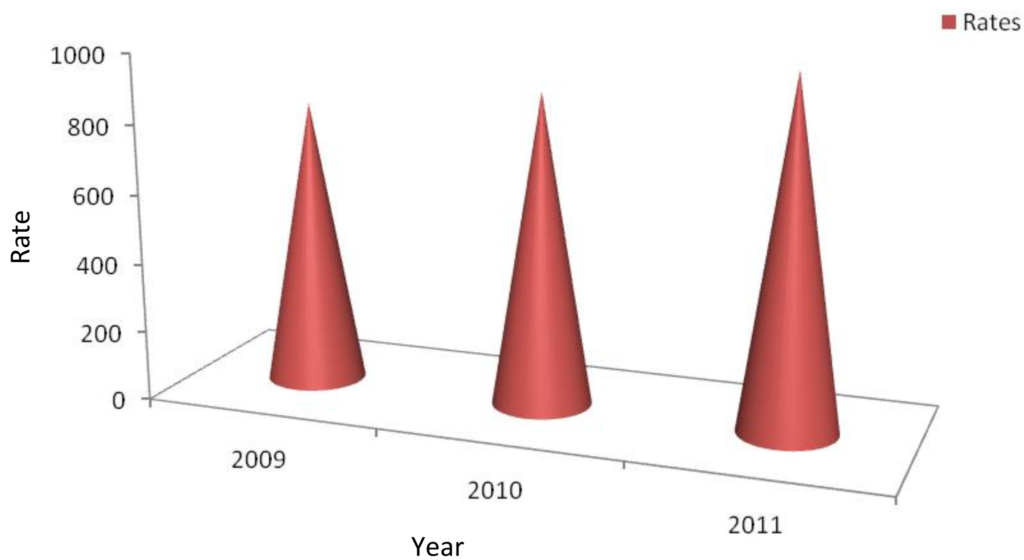

Figure 1. Rates of *Angelica glauca* in Tanakpur mandi for three subsequent years.

medicinal herb for which, beside *in situ* conservation, *ex situ* conservation is also recommended (Vashitha.et.al. 2006). In the temperate and alpine zone of the Himalaya, there is increasing intensity of harvesting of medicinal plants as change in climatic condition have adversely affected the habitats of many species, leading to a gradual loss in regeneration potential and diversity of many economically valuable species. *A. glauca* has been categorized as an endangered species; large scale of cultivation of threatened and economically important wild plants is the most effective way to sustainable utilization and conservation of biodiversity. Propagation occurs by means of seeds and occasionally through rhizome segments (Vashitha.etl.al. 2007, 2009). Only rhizome segment can be used for vegetative propagation. The collectors of raw material may be suggested to use the terminal part of rhizome for cultivation and utilize the remaining root part for medicinal purpose. Considering the economic potential of these species, the technology has significant value for both conservation and

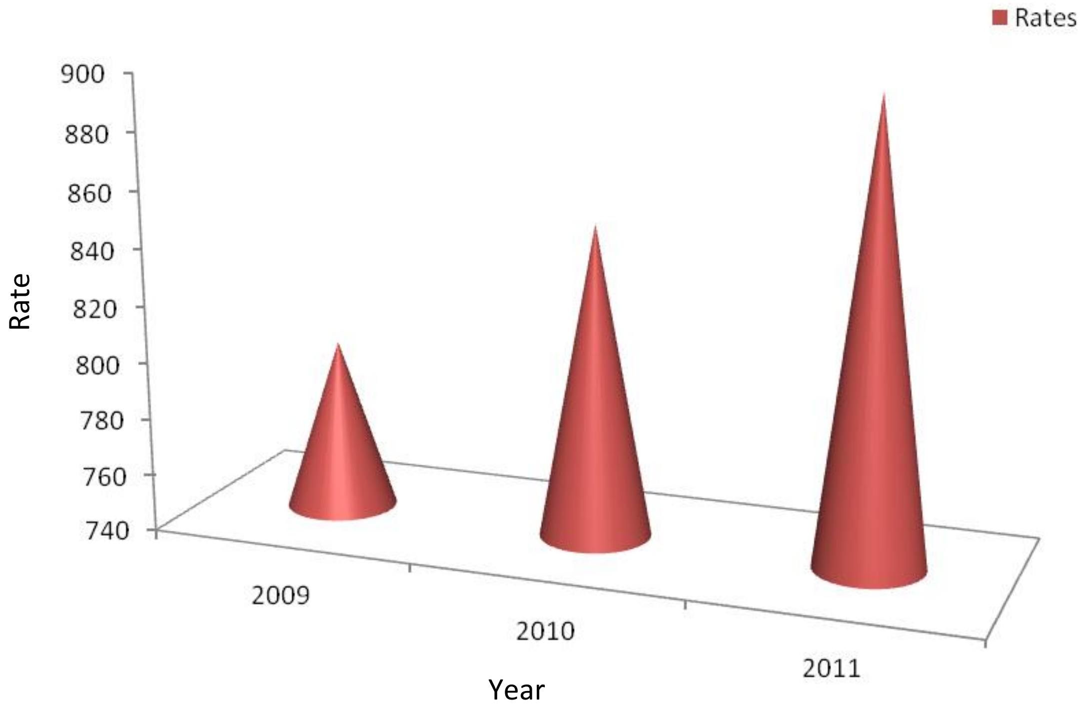

Figure 2. Rates of *Angelica glauca* in Pithoragarh mandi for three subsequent years.

Figure 3. Roots of *A.glauca.*

sustainable utilization of *A. glauca*.

Conclusion

Occasionally, adulteration is prone to occur with expensive materials and with those in short supply. Practically, the phenomenon of adulteration indicates the admission of impurities or removal of all valuable position of the drug or it may be an addition of low grade of spoiled drug with the genuine one; as in *A. archangelica, P. angelicoides* are mixed with *A. glauca* because of low population and apparently these plants roots have same appearance and odour. On account of frequency, density, TBC and IVI, *A. glauca* is an endangered plant in the Kumaon Himalayas. *A. glauca* is with sparse population

Figure 4. Roots of *A. archangelica.*

Figure 5. Habitat photograph of *A. glauca.*

in few areas and is in high demand; to reach the demand adulteration was done. The study also revealed that the natural distribution of the *A. glauca* narrows down due to habitat destruction. Due to excessive and illegal exploitation, these are no longer found in the accessible habitats in large quantities. Exploitation of *A. glauca* is going on, and it is facing severe threats hence it was assigned the endangered status. Considering the economic potential of this species, using the terminal part of rhizome for cultivation by farmers have significant value for both conservation and sustainable utilization of *A. glauca*.

Conflict of Interest

The authors have not declared any conflict of interests.

Figure 6. *Pleurospermum angelicoides.*

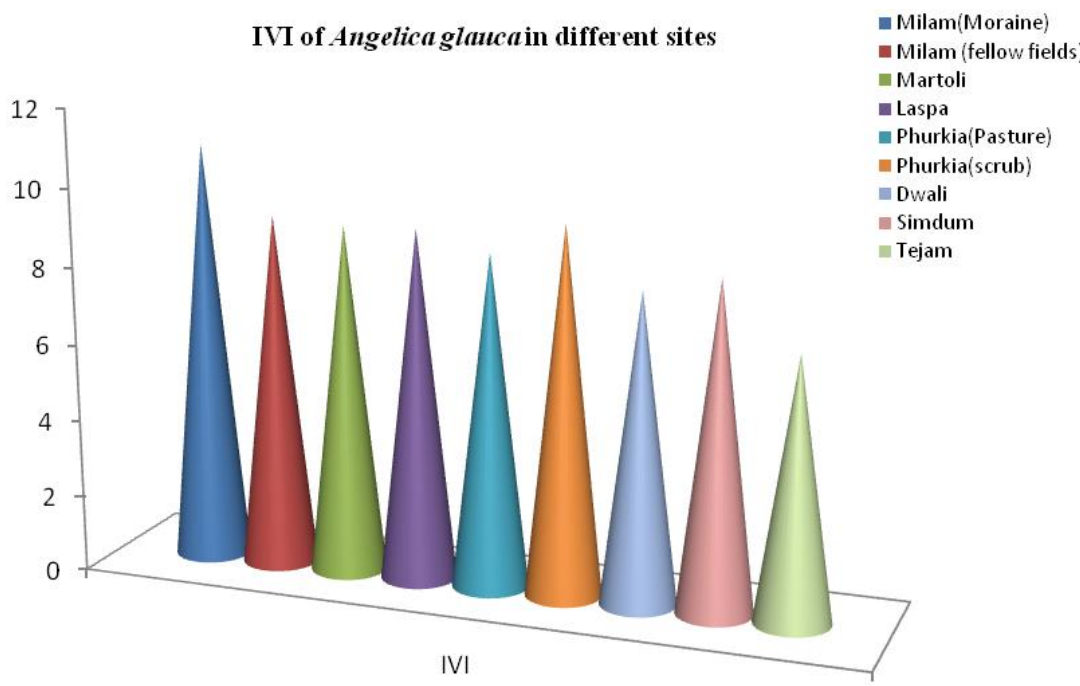

Figure 7. IVI of *Angelica glauca* Edgew in various sites.

ACKNOWLEDGEMENTS

Authors are grateful to Director General, CCRAS, New Delhi and Head, Botany, D.S.B. Campus, Kumaon University, Nainital for providing necessary facilities during the tenure of the work.

REFERENCES

Anonymous (1948).The Wealth of India Vol. I, CSIR, Delhi. P. 79.
Anonymous (1982). Pharmacognosy of indigenous drug, CCRAS, New Delhi.
Anonymous (1985). Index Kewensis Oxford University Press, Amen House, London E.C.4.

Arya D, Joshi GC, Tewari LM (2012). Status and trade of crude drugs in Uttarakhand. J. Med. Plant Res. 6(18):3434-3444.

Arya D, Bhatt D, Kumar R, Tewari LM, Kishore K, Joshi GC (2013). Studies on natural resources, trade and conservation of Kutki (*Picrorhiza kurroa* Royle ex Benth., Scrophulariaceae) from Kumaun Himalaya. Sci. Res. Essays 8(14):575-580.

Bisht NS, Gera M, Sultan Z, Gusain MS (2008). Status of collection, cultivation and marketing of medicinal and aromatic plants in Pithoragarh Uttarakhand. India. Forester 131:346-357.

Chopra RN, Nayar SL Chopra IC (1956). Glossary of Indian medicinal plants, Publication and information Directorate, CSIR, New Delhi.

Bhatt D, Joshi GC, Kumar R, Tewari LM (2014). Phytosociological features and threat categorization of *A. heterophyllum* Wall.ex Royle and *A. ferox* Wall. ex Ser. in Kumaun Himalaya. J. Ecol. Nat. Environ. 6(3):111-118.

Bhatt D, Joshi GC, Kumar R, Tewari LM (2014). Successive variation in phyto-sociological aspects and threat categorization of *Picrorhiza kurroa* Royle ex Benth. in Kumaun Himalaya of Uttarakhand. J. Med. Plant Res. 8(23):829-833.

Mishra R (1968). Ecology Workbook. Oxford and IBH Calcutta.

Rawat GS (2005). Alpine meadows of Uttaranchal, Abhimanyu Gahlot for M/S Bishen Singh Mahendra Pal Singh, Dehradun 248001, India.

Samant SS, Dhar U, Palni LMS (1998). Medicinal Plants of Himalaya: Diversity Distribution Potential Values. Gyanodaya Prakashan, Nainital. HIMAVIKAS Publ. No. 13.

Sarin YK (2008).Principal Crude Herbal Drug of India Bishan Singh Mahendra Pal Singh and Y. K. Sarin, P. 358.

Shah NC, Joshi MC (1970). Folklore Aromatic plant of Kumaon Hills, The flavor industry.

Vashitha RK, Nautiyal BP, Dec MC (2006). Conservation status and morphological variation between population of *Angelica glauca* Edgew and *A. archangelica* Linn. in Garhwal Himalaya. Curr. Sci. 91:1537-1542.

Vashith RK, Nautiyal BP, Nautiyal MC (2007). Economic viability of cultivation of the Himalayan herb *Angelica gla*uca Edgew at different Agro climatic zones. Curr. Sci. 93:1141-1145.

Vashistha RK, Chaturvedi AK, Nautiyal BP, Nautiyal MC (2009). vegetative propagation of *Angelica glauca* Edgew and *A. archengelica* Linn. Two high value medicinal and aromatic herbs of the Himalaya. Nature Sci. 7:8.

Ved DK, Kinhal GA, Ravi K, Prabhakaran V, Ghate U, Vijaya S, Rand IJH (2003). Conservation assessment and management prioritization for the medicinal plants of Jammu and Kashmir, Himachal Pradesh and Uttaranchal. Foundation for revitalization of local Health Traditions, Banglore, India.

academicJournals

Vol. 10(2), pp. 71-78, 30 January, 2015
DOI: 10.5897/SRE2014.5929
Article Number:2A15B5A49797
ISSN 1992-2248
Copyright©2015
Author(s) retain the copyright of this article
http://www.academicjournals.org/SRE

Scientific Research and Essays

Full Length Research Paper

Effect of the aging process on mechanical properties and machinability in AA6013 aluminum alloys

Birol Akyüz* and Safa Şenaysoy

Department of Mechanical and Manufacturing Engineering, Bilecik Seyh Edebali University, 11200 Bilecik, Turkey.

Received 14 April, 2014; Accepted 25 November, 2014

This study investigated the effects of aging process on the mechanical properties and machinability in AA6013 aluminum alloy. To this end, AA6013 aluminum alloy samples were maintained in heat treatment furnace at 530°C (for 8 h) and placed in hot water (at 70°C), and then subjected to aging process by storing in heat treatment furnace (at 180°C) for various times (1, 3, 6, 9, 12 and 24 h). Changes in mechanical and machinability properties of samples that underwent aging process were investigated. At the end of the aging process, an increase was observed in mechanical properties of AA6013 alloy. Cutting forces increased during the machining of alloy depending on the increase in aging time. High mechanical properties were obtained at the end of the 6-h aging process of AA6013 aluminum alloy. A significant increase was observed between mechanical properties obtained at the end of the 6-h aging time and machinability properties with values obtained at the end of the 24th hour.

Key words: Machining, aging, AA6013 aluminum alloys, mechanical properties.

INTRODUCTION

The fact that aluminum alloys have such characteristics as being able to develop low density, high specific resistance, high corrosion resistance and mechanical properties, ease of forming and machining enabled creation of areas of use in various sectors. Of these sectors, automotive, transportation, aviation-aeronautics, electronics, machinery, and manufacturing are the leading ones. They are especially important for achieving fuel savings by reducing weight due to being lightweight and in the prevention of air pollution (Florea et al., 2012; Chen et al., 2012; Bakavos and Prangnell, 2010; Siddiqu et al., 2000; Hayat, 2012).

Another important characteristic of aluminum alloys is that the mechanical properties are open to improvement. Depending on the improvement of the mechanical properties of these alloys, numerous areas of use appear. Aging process is quite important in the improvement of mechanical properties of aluminum alloys. Aluminum alloys are named after the alloy elements they contain. One of the aluminum alloys with most widespread areas of use is 6xxx (containing Aluminum-Al, Magnesium-Mg, and Silicon-Si).

As a result of our literature review, some the studies conducted on 6xxx aluminum alloys are as follows.

In a study by Öztürk et al. (2010), AA6061 aluminum alloys were reported to reach maximum hardness value

*Corresponding author. E-mail: birol.akyuz@bilecik.edu.tr, birolakyuz@gmail.com Tel: +90 228 214 15 42. Fax: +90 228 214 12 22.

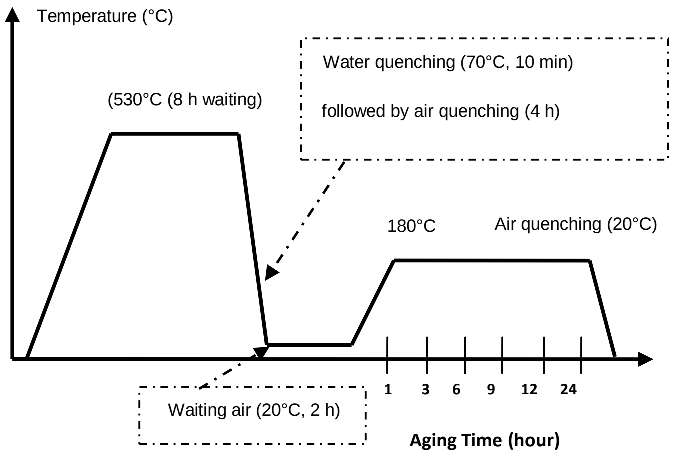

Figure 1. Schematic representation of the aging treatment procedure.

at the end of aging process at 200°C (for 600 min). In a study conducted by Graznya Mrowka-Nowotnik et al. (2005), changes in mechanical properties of AA6005 and AA6082 alloys were investigated under different cooling conditions. They reported that the highest hardness was obtained by cooling in oil. In a study by Meyveci et al. (2010), aging process applied on AA6063 alloy was reported to improve mechanical properties and wear resistance. In their study, Barbosa et al. (2006) investigated mechanical and welding properties of aged 6013 and 6061 alloys. No decrease was reported in mechanical properties following the welding process in 6013 alloy and that the welding property was better. Braun (2006) applied aging process (between 3-100 h, up to 191°C) and investigated tensile, corrosion, and thermal properties of AA6013 alloy. Corrosion resistance of the alloy was reported to increase at the end of aging process. Petroyiannis et al. (2004) examined the effect of corrosion on mechanical properties in 6013 alloy. They reported a reduction in mechanical properties of alloys exposed to corrosion. In a study by Tesch et al. (2007), crack formation of 6013 alloy was investigated by performing fatigue and notch impact tests. Studies reported formation of Mg_2Si intermetallic phases in the microstructure in aging processes of aluminum alloys due to the effect of Mg and Si in alloys. It was suggested that corrosion resistance and strength of alloy increased thanks to the formation of these phases (Zander, 2010; Khalid et al., 2010). In a study by Demir and Gündüz (2009), the effect of aging process on the machinability of AA6061 aluminum alloy was investigated. Cutting forces of aged samples were reported as higher at lower cutting speeds.

Machinability, as a concept, demonstrates the ease or difficulty of the machining of a material in the desired shape, size, and surface quality (Stephenson and Agapiou, 2006; Boothroyd and Knight, 2006). Of the leading properties affecting the machinability of a material, mechanical properties and machining parameters take the lead. They have impact on the cutting forces, surface roughness values, and chip formation occurring during the machining of the material (Kalpakjian and Schmid, 2010; Grover, 2010; Black and Kohser, 2008; Grzesik, 2008).

There is limited number of studies in the literature that investigate the effect of aging process on machinability in AA6013 series aluminum alloys. This study investigated the effects of aging process on the mechanical properties and machinability in AA603 aluminum alloy. Within this scope, changes in mechanical properties of samples that underwent aging process at varying times, their machinability properties, and the correlation between them were investigated.

EXPERIMENTAL PROCEDURE

Mechanical properties

In the experimental study, aging process was applied on AA6013 aluminum alloy samples at varying times. To this end, AA6013 aluminum alloy samples were maintained in heat treatment furnace at 530°C (for 8 h) and placed in hot water (at 70°C), and then subjected to aging process by storing in heat treatment furnace (at 180°C) for different times (1, 3, 6, 9, 12 and 24 h). Aging process was carried out in heat- and time-controlled heat treatment furnace (Protherm 1200°C). Samples were placed in specially designed shelves inside the heat treatment furnace. Samples used in the experiment underwent aging process at times and temperatures noted in Figure 1. Mechanical tests and machinability tests of these samples that underwent aging process were performed. Aging procedures implemented in the experiment are given in Figure 1 and chemical composition of the alloy used is shown in Table 1. AA6013 aluminum alloy samples used in the experiment (24 mm in diameter and 6 m in length) were supplied by Tuncel Metal AŞ.

Hardness tests were conducted in the experimental study. Surfaces of samples used in hardness tests were cleaned by grinding (ranging from 200 up to 1200 grit) (after turning in 15 mm diameter and 12 mm thickness). Hardness test data were obtained by conducting surface measurements (by averaging 10 measurements). Hardness tests were carried out by a Vickers Hardness (HV_{10}) (Shimadzu HMV-2) testing device. Hardness values were established by averaging data (by conducting at least 10 measurements).

In the experimental study, such mechanical tests as Ultimate Tensile Strength (UTS), Yield Strength (YS) and Elongation % (EL%) of samples that underwent aging process were carried out. Samples used in mechanical tests were prepared as per ASTM-E8 standard (10 samples each). By averaging the data obtained from these samples (10 samples from each different aging time), test data were obtained on ultimate tensile and yield strengths and elongation. These tests were conducted at room temperature (20ºC) at 2.5 mm min^{-1} crosshead speed (Shimadzu Autograph AGS-J 10 kN Universal Tester).

Machining properties

In this study, data were obtained on cutting forces by keeping the

Table 1. Chemical composition of the studied AA6013 aluminum alloy (*Wt %).*

Parameter	Fe	Si	Cu	Mn	Mg	Zn	Ti	Cr	Al
AA6013	0.5	1.0	0.8	0.5	0.9	0.1	0.1	0.1	Rest

Table 2. Machining parameters and conditions used during the test.

Parameter	Depth of cut DoC (mm)	Cutting speed V_c (m/min)	Aging temperature (°C)	Aging time (h)
AA6013	0.10, 0.25, 0.50	60, 120, 180	180°C	1, 3, 6, 9, 12, 24

chip section fixed at varying cutting speeds on AA6013 aluminum alloy samples that underwent aging process at varying times. During the application, the machinability of alloys were investigated by examining the changes in cutting forces (at varying cutting speeds and varying depths of cut) depending on the aging time.

A DMG Alpha 300 CNC turning lathe was used in machinability experiments. Data were obtained under dry machining conditions and vertical processing method. A Polycrystalline Diamond (PCD) (CCGT 120408 FL K10) was used as the cutting edge in the experiments. Surface roughness values of samples (Ra-µm) were measured by a surface roughness measuring device (TIME TR200). Data on cutting forces were obtained from a specially designed strain gauge (Figure 2).

After the cleaning chip was removed from the surfaces of samples used in the experiment (20 mm in diameter), data on cutting forces were obtained. Data on cutting forces obtained from the experiment were classified according to aging times, and graphs were prepared. Machining parameters used in the experimental study are given in Table 2.

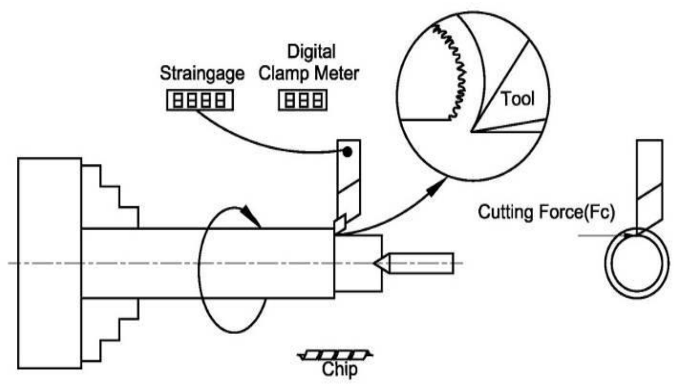

Figure 2. Schematic representation of experimental set-up with strain gauge.

EXPERIMENTAL RESULTS AND DISCUSSION

Mechanical properties

Hardness values obtained as a result of aging process of AA6013 aluminum alloy are given in Figure 3. Depending on the aging time, an increase was observed in hardness values of AA6013 alloy. As can be seen in Figure 3, mean hardness values were measured in unaged reference sample as 51.5 HV_{10}, in samples aged for 6 h as 130.2 HV_{10}, in samples aged for 12 h as 132.4 HV_{10}, and in samples aged for 24 h as 138.1HV_{10}. Hardness of the unaged sample demonstrated a vast increase at the end of 6-h aging (over 2.5 times). A major difference was not observed between the hardness values obtained at the end of 6-h and 24-h aging times (~5%). As a result of the study, it was observed that the hardness value of alloy increased parallel to the aging time. The hardness increase in alloy as a result of aging process may be explained by phases formed within the microstructure, precipitation, and change in grain sizes.

Figure 3. Hardness values obtained at various aging times of AA6013 alloy.

Data on ultimate tensile strengths (UTS), Yield Strengths (YS) and Elongation % (EL%) amount of AA6013 aluminum samples that underwent aging process in the study are given in Figure 4 and 5. When

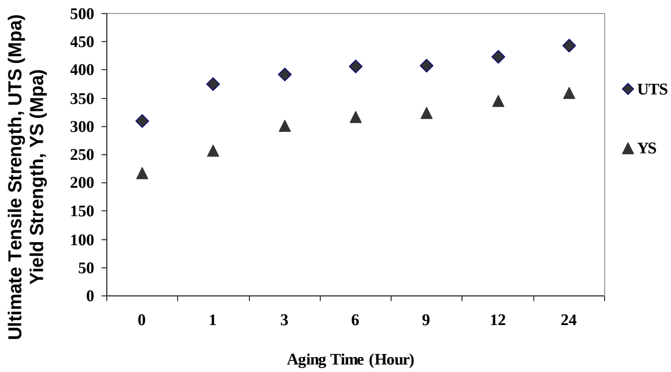

Figure 4. Tensile and yield strength values obtained from various aging times in AA6013 alloy.

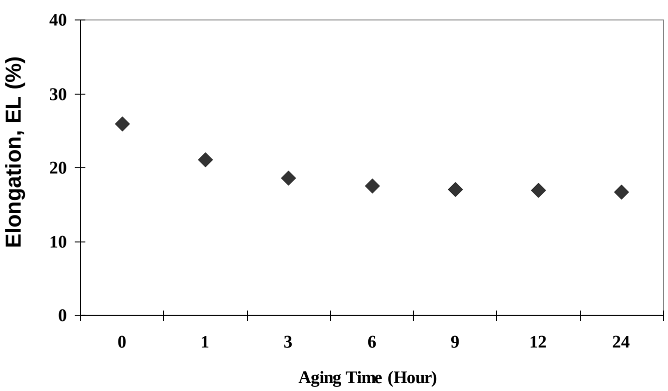

Figure 5. Elongation % values obtained from various aging times of AA6013 alloy.

examined the UTS and YS values of samples in Figure 4, the obtained values were 309.3 MPa UTS and 216.9 MPa YS in unaged reference sample, 410.6 UTS and 316.9 YS in the samples aged for 6 h, 422.7 UTS and 340.8 YS in samples aged for 12 h, and 442.4UTS and 352.5YS in samples aged for 24 h. While a major increase was observed in UTS and YS values of unaged sample at the end of 6-h aging (~32%), a significant increase was not found after 6 h. A significant difference was not observed in the experiment between UTS and YS values obtained at the end of 6-h and 24-h aging (~7%). When examined Figure 5, while the highest EL% value obtained in the experiment was from the unaged reference sample (25.9%), it was 17.4% for the sample aged for 6 h, 16.9% for the sample aged for 12 h, and 16.5% for the sample aged for 24 h. It was observed from the experimental study that UTS and YS values of the alloy increased due to the rise in aging time in AA6013 alloy subjected to the aging process while the elongation % value saw a decrease. These results are in accordance with the literature.

Machining properties

Data on cutting forces obtained from the machining of AA6013 aluminum alloy that was implemented aging process in the experimental study are given in Figure 6a to c. When examined Figure 6a to c, an increase was observed in the cutting forces of the alloy depending on the rise of aging time. Similarly, cutting forces increased depending on the depth of cut.

When analyzed the cutting forces formed depending on the aging times of alloy in Figure 6a, it was measured at 60 $m.min^{-1}$ cutting force (DoC:0.5mm) as 30.7 N in unaged reference sample, 51.9 N in the sample aged for 6 h, 52.4 N in the sample aged for 12 h, and 53.8N in the sample aged for 24 h. In Figure 6a, it was measured at 180 $m.min^{-1}$ cutting force (DoC:0.5 mm) as 21.4 N in unaged reference sample, 43.6 N in the sample aged for 6 h, 44.1 N in the sample aged for 12 h, and 45.7 N in the sample aged for 24 h. When compared the cutting forces obtained from the unaged reference sample and cutting forces measured from samples that were implemented a 6-h aging process, an increase over 70% was observed in cutting forces at the end of 6 h (Figure 6a). On the other hand, when compared the cutting forces obtained from the sample that was aged for 6 h and the sample aged for 24 h, a significant difference was not observed (max.0.2%) between them. From this point of view, it may be noted that the highest cutting force was reached in samples that were implemented a 6-h aging process.

When Figure 6a to c was analyzed, it was observed that cutting forces decreased along with the rise in cutting speed in all samples that underwent aging process (Figure 6a to c). While the highest cutting force in all samples that were implemented aging process (at all depths of cut) occurred at 60 $m.min^{-1}$ cutting speed, the lowest cutting force was obtained at 180 $m.min^{-1}$ cutting speed. Cutting forces increased along with rises in depths of cut in all samples that underwent aging process (Figure 6a to c). The highest cutting force at all depths of cut and at all cutting speeds was reached in samples aged for 6 h. From this viewpoint, when compared the machinability of unaged reference sample and samples aged for 6 h, the machinability of samples aged for 6 h became difficult (above ~70%). However, a significant difference was not observed between the machinability of samples aged for 6 h and samples aged for 24 h (~0.2%).

In the experimental study, it was observed in AA6013 aluminum alloy that the cutting forces occurred at 60 $m.min^{-1}$ cutting speed were higher compared to cutting forces obtained at a cutting speed of 180 $m.min^{-1}$ (Figure 6a to c). In the light of this, the reason for higher cutting

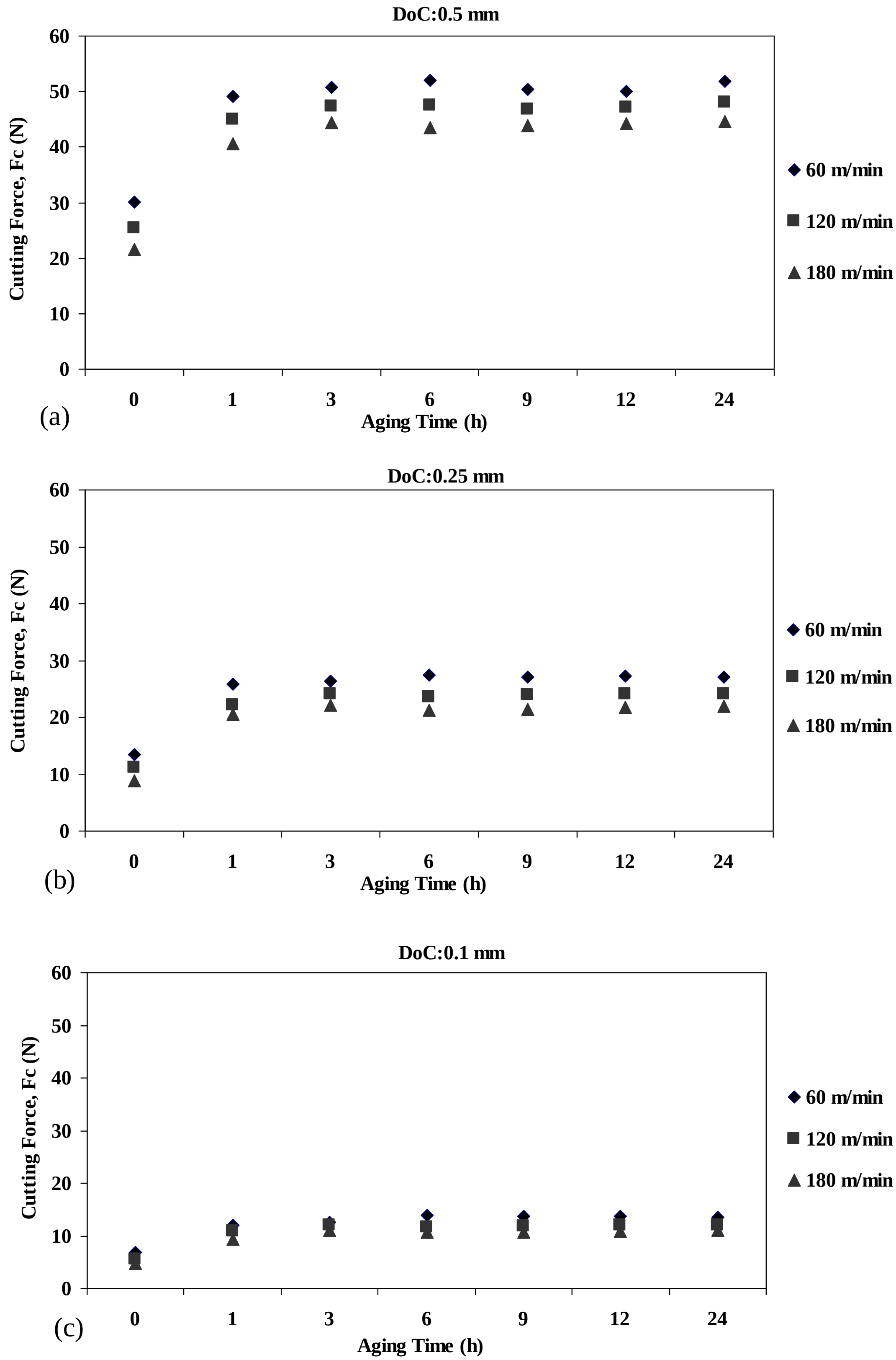

Figure 6. Cutting speeds obtained at different aging times in AA6013 alloy (F_C) (DoC: (a) 0.5 mm (b) 0.25 mm and (c) 0.1 mm respectively.

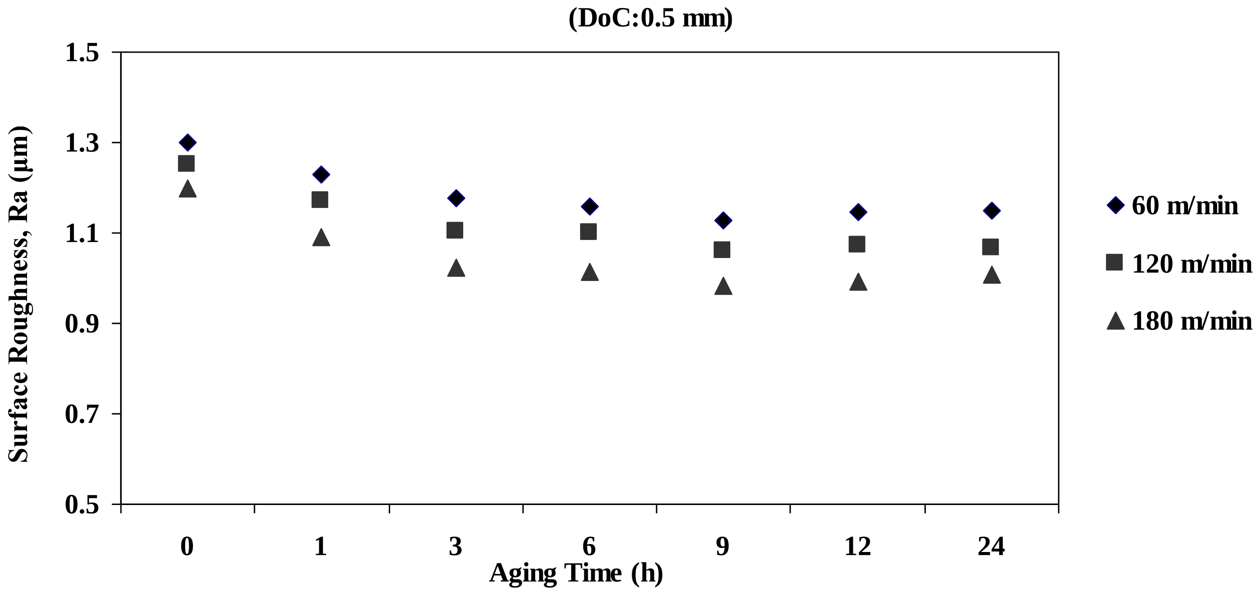

Figure 7. Surface roughness values obtained from various aging times of AA6013 alloy (R_a) (DoC:0.5 mm).

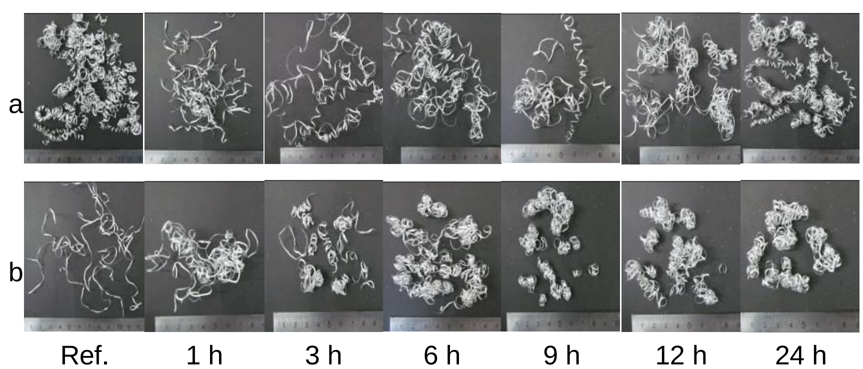

Figure 8. Chip images formed at varying aging times in AA6013 alloy and at a) 60 $m.min^{-1}$ and b) 180 $m.min^{-1}$ cutting speed (DoC:0.5 mm).

forces at lower cutting speeds in AA6013 alloy is due to work hardening depending on dislocation deposit at the time of cutting. The fact that the movement of dislocations is difficult against plastic deformation at lower cutting speeds (lower revolutions) causes an increase in cutting forces.

Surface roughness values measured on experimental samples machined in the experiment (at 0.5 mm depth of cut) are given in Figure 7. It was observed that surface roughness values dropped along with the increase in cutting speed while machining the samples at all aging times. Therefore, the highest surface roughness value at all aging times appeared at 60 $m.min^{-1}$ cutting speed. An increase was observed in cutting forces as a result of chips depositing on the cutting surface at lower cutting speeds. It may be noted that, since deposit chip was formed, this caused surface roughness values to increase (Stephenson and Agapiou, 2006; Boothroyd and Knight, 2006; Kalpakjian and Schmid, 2010; Grover, 2010).

Chip images obtained from the machining of AA6013 alloy subjected to aging process are given in Figure 8. Analysis of chip images reveals a shortening in chip lengths depending on the increase in aging time. Similarly, a shortening occurred in chip lengths depending on the increase in cutting speed. A continuous chip formation occurs along with deposit chip formation at lower cutting speeds and chips are formed by ductile fracture, and elongation occurs in chip lengths. Surface roughness values increased thanks to this deposit chip. Longer chips at lower cutting speeds might be interpreted as the occurrence of ductile fractures (Kalpakjian and Schmid, 2010; Grover, 2010; Black and Kohser, 2008; Grzesik, 2008). Shortening of chip lengths thanks to an increase in cutting speed may be explained by the formation of a more brittle structure as a result of a rise in the hardness of alloy (Figure 8). A gradual shortening is observed in chip lengths due to the formation of a more brittle structure. From this point of view, AA6013 alloy that was implemented an aging process may be noted to become gradually brittle depending on the increase in aging time of samples (Figure 8). Data obtained in this section are in accordance with the data from mechanical tests in the experimental study (Figures 3 to 5.).

Depending on the aging time, an increase was observed in mechanical properties of the alloy. This increase in the mechanical properties had an impact on the machinability properties of alloys. Due to the differences in fine precipitations formed in the alloy depending on the aging process, hardness and strength results were also believed to be different. Since fine precipitations formed within grain in alloy following aging process hampered or prevented the movement of dislocations during deformation, an increase was observed in mechanical properties (hardness, yield and tensile strengths). From this point of view, the reason for higher cutting forces at lower cutting speeds in AA6013 alloy stems from work hardening due to dislocation deposit during cutting. The fact that dislocation movement being difficult against plastic deformation at lower cutting speeds (lower revolutions) causes an increase in cutting forces (Stephenson and Agapiou, 2006; Grzesik, 2008).

Conclusions

This experimental study investigated the effects of aging process on the mechanical properties and machinability in AA603 aluminum alloy. Results obtained from the experimental study are as follows:

1) At the end of the aging process, such mechanical properties as hardness (HV), UTS, and YS of AA6013 alloy increased due to aging time. However, elongation % value (EL%) decreased depending on the increase in aging time. The alloy reached higher mechanical properties at the end of 6-h aging time. A significant difference was not observed between UTS and YS values obtained at the end of 6-h aging and 24-h aging (~7%). Similarly, in hardness value, a significant difference was not established between the hardness values obtained at the end of 6-h and 24-h aging times (~5%).

2) A decrease was observed in cutting forces as the cutting speed rose. The highest cutting forces occurred at the lowest cutting speed. The reason for high cutting forces at lower cutting speeds (lower rotations per minute) is due to work hardening depending on dislocation deposit at the time of cutting. Therefore, cutting forces occurred at 60 $m.min^{-1}$ cutting speed were higher compared to those occurred at 180 $m.min^{-1}$ cutting speed.
3) Since cutting forces increased depending on the rise in aging time, machinability of the alloy demonstrated a decrease depending on the aging time.
4) Cutting forces increased as the depth of cut rose. The highest cutting forces occurred in 0.5 mm depth of cut and at 60 $m.min^{-1}$ cutting speed. Surface roughness values improved depending on the aging time and cutting speed increases.

Conflict of Interest

The authors have not declared any conflict of interests.

ACKNOWLEDGEMENT

A heat treatment furnace that was purchased within the scope of a project conducted by the author (Bilecik S.E. University, BAP: 2012–01 BİL.03-02) was used in this study.

REFERENCES

Bakavos D, Prangnell PB (2010) Mechanisms of joint and microstructure formation in high power ultrasonic spot welding 6111 aluminium automotive sheet. Mater. Sci. Eng. A 527:6320–6334.
Barbosa C, Dille J, Delplancke JL, Rebello JMA, Acselrad O (2006). A microstructural study of flash welded and aged 6061 and 6013 aluminum alloys, Mater. Characteriz. 57:187-192.
Black JT, Kohser RA (2008). Materials and Processes in Manufacturing (10th Ed.), John Wiley & Sons, Inc.
Boothroyd G, Knight WA (2006). Fundamentals of Machining and Machine Tools, (3rd Ed.), Taylor & Francis.
Braun R (2006). Investigations on the long-term stability of 6013-T6 sheet. Mater. Characteriz. 56:85–95.
Chen YC, Bakavos D, Gholinia A, Prangnell PB (2012). HAZ development and accelerated post-weld natural ageing in ultrasonic spot welding aluminium 6111-T4 automotive sheet. Acta Materialia 60:2816–2828.
Demir H, Gündüz S (2009). The effects of aging on machinability of 6061 aluminium alloy. Mater. Des. 30:1480–1483.
Florea RS, Solanki KN, Bammann DJ, Baird JC, Jordon JB, Castanier MP (2012). Resistance spot welding of 6061-T6 aluminum: Failure loads and deformation. Mater. Des. 34:624–630.
Grover MP (2010). Principles of Modern Manufacturing (4th Ed.), John Wiley & Sons, Inc.
Grzesik W (2008). Advanced Machining Processes of Metallic Materials, Elsevier, UK.
Hayat F (2012). Effect of aging treatment on the microstructure and mechanical properties of the similar and dissimilar 6061-T6/7075-T651 RSW joints, Mater. Sci. Eng. A 556:834-843.

Kalpakjian S, Schmid SR (2010). Manufacturing Engineering and Technology, Prentice Hall.

Khalid RH, Ram GDJ, Phanikumar G, Rao KP (2010). Microstructure and tensile properties of friction welded aluminum alloy AA7075-T6. Mater. Des. 31:2375-2380.

Meyveci A, Karacan İ, Çalıgülü U, Durmuş H (2010). Pin-on-disc characterization of 2xxx and 6xxx aluminium alloys aged by precipitation age hardening. J. Alloys Compounds 491:278–283.

Mrowka-Nowotnik G, Sieniawski J (2005). Influence of heat treatment on the microstructure and mechanical properties of 6005 and 6082 aluminium alloys. J. Mater. Process. Technol. 162–163:367–372.

Öztürk F, Sisman A, Toros S, Kilic S, Picu RC (2010) Influence of aging treatment on mechanical properties of 6061 aluminum alloy. Mater. Des. 31:972–975.

Petroyiannis PV, Kermanidis AT, Papanikos P, Pantelakis SG (2004). Corrosion-induced hydrogen embrittlement of 2024 and 6013 aluminum alloys. Theor. Appl. Fracture Mech. 41:173–183.

Siddiqu RA, Abdullah HA, Al-Belushi KR (2000). Influence of aging parameters on the mechanical properties of 6063 aluminium alloy. J. Mater. Process. Technol. 102:234-240.

Stephenson DA, Agapiou JS (2006). Metal Cutting Theory and Practice (2.nd Ed.), Taylor & Francis.

Tesch A, Pippan R, Trautmann KH, Döker H (2007). Short cracks initiated in Al 6013-T6 with the focused ion beam (FIB)-technology. Int. J. Fatigue 29:1803-1811.

Zander J, Sandström R (2008). One parameter model for strength properties of hardenable aluminium alloys. Mater. Des. 29:1540–1548.

academicJournals

Vol. 10(2), pp. 79-85, 30 January, 2015
DOI: 10.5897/SRE2014.6025
Article Number:769F19C49799
ISSN 1992-2248

http://www.academicjournals.org/SRE

Scientific Research and Essays

Full Length Research Paper

Assessment of non-ionizing radiation from radio frequency energy emitters in the urban area of Natal City, Brazil

Fred Sizenando Rossiter Pinheiro[1]*, Técia Maria de Oliveira Maranhão[2], Mário Bernardo Filho[3], Márcio Eduardo da Costa Rodrigues[1], Gutembergue Soares da Silva[1], Thiago Palhares de Sousa[1], Manuel Antonio Bouzas Sanchis[1], André Luiz Severiano Câmara[1], João Paulo da Silva Gonçalo[1] and Andrei de Abiahy Carneiro da Cunha Braga[1]

[1]Departamento de Engenharia de Comunicações, Universidade Federal do Rio Grande do Norte, Campus Central, Av.Sen. Salgado Filho 3000, Caixa Postal 1524, Lagoa Nova, Natal, CEP 59078-970 - Christmas -RN – Brazil.
[2]Departamento de Toco-Ginecologia ,Universidade Federal do Rio Grande do Norte, Brazil.
[3]Instituto de Biologia Roberto Alcântara Gomes, Universidade do Estado do Rio de Janeiro, Av. 28 de Setembro 87 fundos, Brazil.

Received 25 June, 2014; Accepted 12 January, 2015

The massive increase of wireless communications in the world calls for responsible actions by governments in order to prevent possible health hazards. In addition to cellular towers overcrowding in urban areas, it is also important to consider other radio frequency radiations from different sources. The electric field intensity is one of the fundamental parameters to assess the exposure of human beings to Non-Ionizing Radiation (NIR). In this study, all main non-ionizing radiation sources in the urban area of Natal, Brazil (a city of about 860.000 inhabitants) were located and characterized with respect to frequency band, telecommunications service and integrated electric field strength. Measurements of far electric field intensity with frequency ranging from 30 MHz to 3 GHz were made in a survey of 140 outdoor points spread across all the 167.26 km^2 area of the city. The results obtained have made it possible to draw a map of the regions of the city according to different electric field and exposure ratio (ER) intensities. In 71.4% of the sampled outdoor points, the highest exposure ratio measured were originated from TV broadcasting services, 22.1% from Transmissions Cellular Towers and 6.4% from Frequency Modulated Broadcasting.

Key words: Non-ionizing radiation, electric field intensity, TV broadcasting, radio frequency radiation, measurement of radio frequency radiation, propagation in Urban Areas, International Commission on Non-Ionizing Radiation Protection (ICNIRP).

INTRODUCTION

Non-ionizing radiation (NIR) is the radiation in the part of the electromagnetic spectrum below 300 GHz where there is insufficient energy to cause ionization (ANATEL, 2002). The United Nations Conference on Environment and Development held in 1992 in Rio de Janeiro established the Precautionary Principle which has become the basis for environmental policies carried out by many countries, besides being the landmark for the structuring of the Environmental Law.

The Precautionary Principle is part of Principle 15 of the Declaration of Rio (2013) and states that “In order to protect the environment, the precautionary approach shall be widely applied by States according to their capabilities. Where there are threats of serious or irreversible damage, lack of full scientific certainty shall not be used as a reason for postponing cost-effective measures to prevent environmental degradation”.

Reactive oxygen species (ROS) concentration increase within the cell caused by RF/MW radiation seems to be a biologically relevant hypothesis to give clear insight into the RF/MW action at non-thermal level of radiation (Gotsis et al., 2005).

Environmental protection norms set limits to existing non-ionizing radiation emission and are inspired mainly by documents issued both by the International Commission on Non-Ionizing Radiation Protection (ICNIRP) and the American National Standards Institute (IEEE/ANSI). The limits have been established essentially based on thermal effects of electromagnetic fields, which are well known. Lately, the non-thermal effects of non-ionizing radiation (effects on the nervous, cardiovascular and immune systems, etc.) have been under research, and special attention is being drawn to a World Health Organization (WHO) project which involves scientists from 45 different countries in an attempt to address the issue (ICNIRP, 1998).

The ICNIRP (1998) defined guidelines for limiting exposure to time-varying electric, magnetic and electromagnetic fields. In establishing exposure limits, the commission recognizes the need to reconcile a number of differing expert opinions.

Electromagnetic fields with wavelengths longer than 10 m (frequencies lower than 30 MHz) have interaction properties which differ greatly from those with wavelengths that are approximately equal to or less than the physic dimension of the human body. A radiofrequency band of 0.3-30 MHz, for example, is used in medicine for ablation, coagulation and tissue cauterization (LIN, 2012).

On the other hand, considerable controversy surrounds the possibility of a link between exposure to Extremely Low Frequency (ELF, ranging from 3 to 30 Hz) magnetic fields and an elevated risk of cancer. Although, results suggest that indeed the magnetic field may play a role in the association with leukemia risk, there is uncertainty because of small sample numbers and also due to a correlation between the magnetic field and proximity to power lines (ICNIRP, 1998).

The intensity of the electromagnetic radiation is typically measured by the power density per square meter (w/m²) or by the intensity of the electric field (V/m).

The effects of the absorption of the NIR by human body tissues present distinctive characteristics for different radiation frequencies. On that account, the laws made to limit the exposure to NIR are parameterized by the frequency of the wave operation (Table 1).

Every tissue of the human body has a different energy absorption rate. This energy absorption can be characterized by a parameter known as specific absorption rate (SAR). In practice, there are some difficulties in performing SAR measurements, the most important of them being the difficulty to measure inside the living tissue. Therefore, the radiation measurements in air are accepted. These levels will in general be smaller inside the biological tissue mainly due to attenuation of the radiofrequency energy traveling through various material media (Pérez-Vega and Zamanillo, 2005).

The SAR (especially in the head of mobile phone users) may be simulated using Mathematical methods, for example the Finite Difference Time Domain – FDTD (Salles et al., 2003).

There is a scientific debate on whether or not a long exposition to electromagnetic radiation levels lower than the limits could cause harmful effects on health. Many research projects are involved in this investigation by *in vivo*, *in vitro* and epidemiological studies (Feychting et al., 2005).

Eskander et al. (2012) published a case-study report as follows: “Persons of ages 14–22 years or 25–60 years who were exposed, for time intervals extended to 6 years, to RFR either from mobile phones or from base stations suffered significant decreases in their plasma ACTH and serum cortisol levels as compared to the control group. High significant decrease (Pb0.01) in plasma ACTH and serum cortisol levels was observed for persons exposed to RFR from base stations at distances extended from 20 to 500 m for a period of 6 years as compared to the control group”.

The definition of human exposure limits (ICNIRP, 1998) is the main reference used for ANATEL (2002) in Resolution Number 303 (Table 1). The Federal Law 11.934 (Brazil, 2009) defines minimum distances of at least 50 m from Radio Transmission Stations to “critical areas” (hospitals, schools, asylums, nurseries, clinics).

Measurements of RF level very close to 4 Base Cellular Stations (near field, 5, 15 and 25 m) in Benin City (Nigeria) at frequency 1800 MHz, shows higher values at 15 m away (Black and Henry, 2010).

In Italy (Region Valle d’Aosta), measurements of the electromagnetic fields (EMF) emitted by 3 UMTS base stations have been correlated with network counters related to traffic variation and radiated power in order to obtain a more realistic yet conservative calculation of the

*Corresponding author. E-mail: fredrossiter@uol.com.br, Tel: 055-84)9193-6298.

Table 1. Exposure limits to NIR (General population) ANATEL.

Frequency range	Electric field strength (E) (V/m)	Magnetic field strength (H) (A/m)	Plane-wave equivalent power density (Seq) (W/m2)
9KHz- to 150 KHz	87	5	x
0.15 to 1 MHZ	87	0.73/f	x
1 MHZ to 10 MHz	$87/f^{1/2}$	0.73/f	x
10MHz to 400MHz	28	0.073	2
400MHz to 2000MHz	$1.375\ f^{1/2}$	$0.0037f^{1/2}$	f/200
2GHz to 300 GHz	61	0.16	10

EMF emitted from a UMTS base station. The highest value of power obtained from the data averaged over 6 min was approximately the 75% of the maximum theoretical power that a radio base station can transmit (Bottura et al., 2012).

MATERIALS AND METHODS

In this study, the electric field intensities in the urban area of the city of Natal were measured with a Rohde & Schwarz FSH6 spectrum analyzer connected to an isotropic probe with a frequency range from 30 to 3000 MHz. The probe was fixed to a wooden tripod (1.65 m). A GPS and a notebook computer completed the system in order to run the proprietary software and to communicate with the spectrum analyzer. Three-axis polarization probe measurement in x, y and z and quadratic composition of the fields. Antenna Cable Set (only without connectorization) and short length, provided. Trace Mode / Detector: Max Hold / RMS.

The adopted frequency ranger covers most of the radio broadcasting services, the entire mobile telephony service and the IEEE 802.11 b/g systems. The isotropic probe has directivity close to unity (in linear scale), which means that it receives the signals coming from every direction almost equally, it is controlled by proprietary Rohde & Schwarz software allowing the user to configure the "measurement packets" for each service and therefore to run the entire setup with just a few commands.

Measurements were done preferably at peak mobile telephony times in order to maximize the probability of getting higher signal levels (10.00 am to 12.30 am and 3.00 pm to 7.00 pm), in far-field zone in 140 outdoor points covering all districts including the main streets and the neighborhoods of Cell Towers (including line of sight points), shopping malls, hospitals and schools, defined basically according to population density criteria. The chosen points are at an average distance of 320 m from the nearest tower base station. Figure 1 illustrates the measurements equipments. Figure 2 shows the measurement points in Natal City Area.

The equipment comes with proprietary software designed with some specialized features to perform NIR measurements. Particular characteristics of each service require different measurement packets to be configured. Frequency range, modulation type and transmission dynamics are among the main characteristics affecting measurement setup. Since the interest was in the analysis of EMF radiation from base stations, only the downlink emissions were measured.

The measurement packets of the software were adjusted according to Rhode Schwartz User Manual Instructions to our specific needs (different signal variability for different services and Brazilian service regulation / ICNIRP). The “dwell time” and bandwidths were adjusted according to Table 2. Hardware and software of FSH6 Spectrum Analyzer used are dedicated to this type of measurements. The mean was computed considering all loops and there was measurement uncertainty (mean) of 0.14 dB.

RESULTS

In Urban Area of Natal of September 2014, there were about 875 cellular Base Stations (358 Towers), 18 TV Broadcast Stations, 6 OM and 12 FM Broadcast Radio Stations. Most of the broadcast stations are located at east side of the city.

The highest values for electric field intensity were observed for TV Broadcast Service in 68.6% of the measured points (Table 3). Figure 3 shows the Total (broadband) Electric Fields Intensities in different points. The "exposure ratio" (ER) is one meaningful parameter to be analyzed. It is a quadratic relation between the measured electric field in a specific center frequency and the exposure limit for that frequency (Table 1). The ER is recommended by both ICNIRP (1998) and ANATEL (2002) for this kind of measurement.

$$ER = \sum_i \frac{{E_{m,i}}^2}{{E_{L,i}}^2} \leq 1 \qquad (1)$$

In Equation (1), for each channel centered on frequency i, $E_{m,i}$ is the measured electric field, whereas $E_{L,i}$ is the limit for that frequency according to Table 1. So in the measurement point, the sum of all individual ERs (each one computed using electric field values –measured and limit – for a single frequency) must be less than or equal to the unity (Equation (1), which presents the overall ER). It means that the contribution of the ensemble of services to human exposure to NIR is below or equal to the limit. TV Broadcast Service dominates the ER composition (Table 4).

DISCUSSION

In spite of having about 340 Radio Base Stations Towers spread across the urban area, the Mobile Telephony is not the principal source of non-ionizing electromagnetic radiation in Natal. Radiation from TV Broadcast is the

Figure 1. Measurement equipments near a beach in the city of Natal.

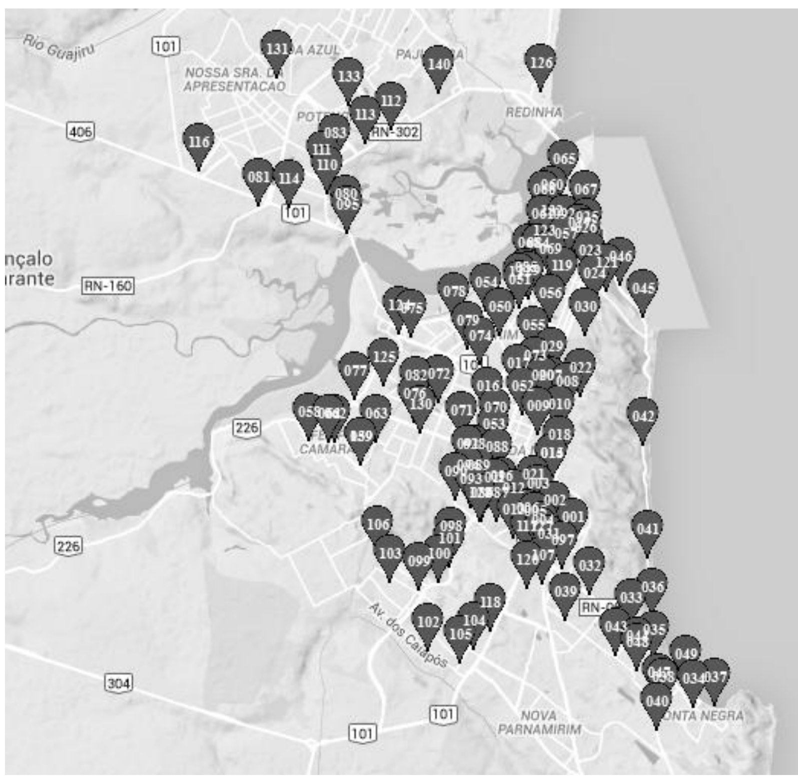

Figure 2. Points of measurements in the urban area of Natal.

Table 2. Configuration of packages (FSH6 S. ANALYZER).

Services / Parameter	TV	FM Radio	Wi-Fi (2,4 GHz)	2G (GSM)	3G(UMTS)
Video BW	Auto	-------	-------	------	------
Dwell time	50 ms	50 ms	5000 ms	1000 ms	50 ms
BW for each central frequency	6 MHz	200 kHz	22 MHz	200 kHz	5 MHz

Table 3. Summary of electric fields measurements.

Service	Mean (V/m)	Highest values* (V/m)	% Highest Values **
TV Broadcast	8.14E-01	6.11E+00	68.6
Mobile Telephony (2G / 3G)	6.25E-01	4.39E+00	27.1
FM Radio Broadcast	2.25E-01	1.35E+00	4.3
WLAN (IE 802.11 bg)	1.83E-01	2.24E-01	0.0

* Maximum for each service in all measured points. ** Percentage in which each service has the greatest electric field compared to other 3 services researched.

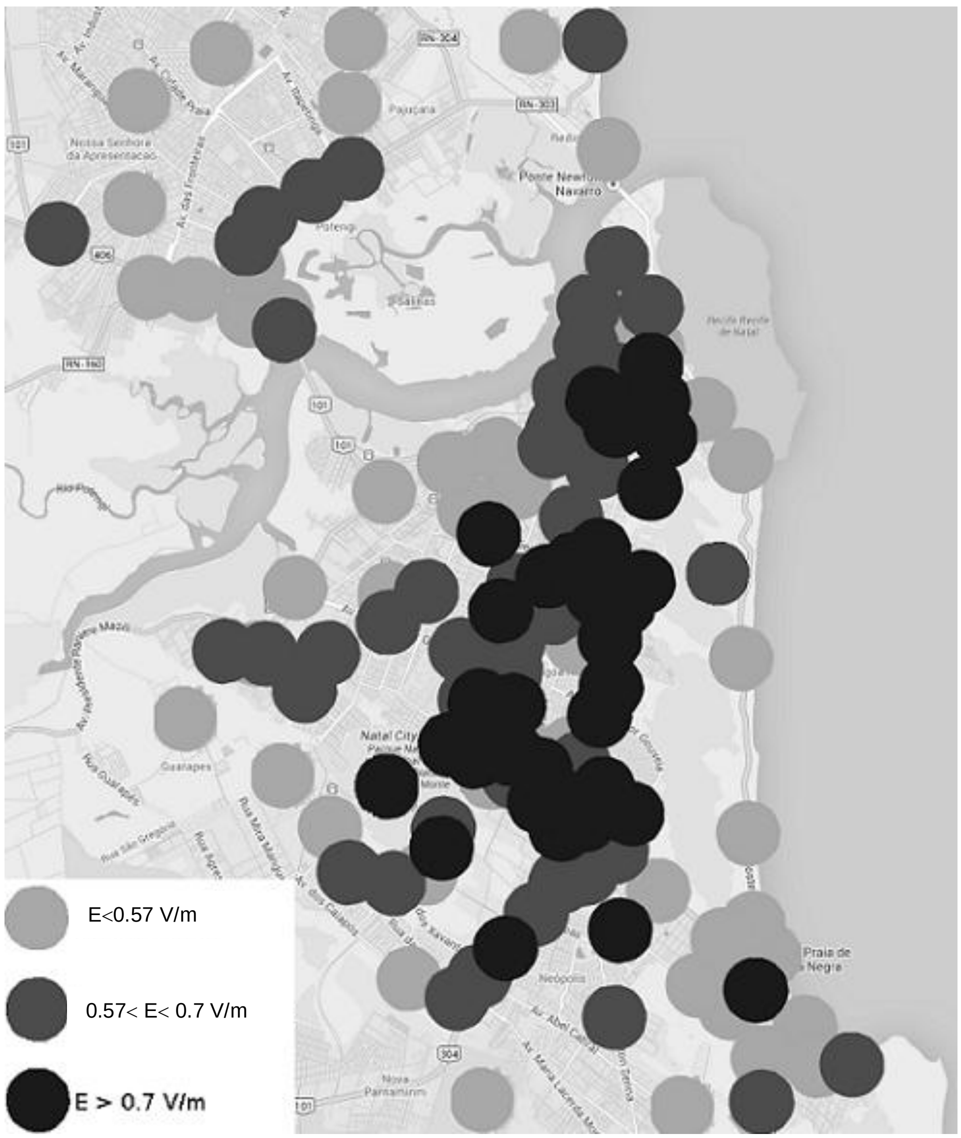

Figure 3. Map of the regions of the city according to different electric fields intensities.

highest in most part of the city.

Non ionizing radiation levels measured in Greece were also significantly below the safety reference levels. Specifically, 90% of the stations have been measuring electric field strength values below 3 V/m (Gotsis et al., 2005).

Table 4. Exposure ratio results.

Service	Mean considering all Points	Highest Values*	% ER Highest Values**
TV Broadcast	2.05E-03	4.77E-02	71.4
Mobile Telephony	5.79E-04	3.29E+00	22.1
FM Broadcast	1.35E-04	1.12E+00	6.5
WLAN (IE 802.11bg)	1,07E-05	1.35E-05	0.0

* Maximum for each service in all measured points. ****** Percentage in which each service has the great ER compared to other 3 services.

Measurements at Sakarya Maltepe in Turkey results to highest reading of electric field strength for FM Radio Services and the highest reading was 2.19 V/m (Tesneli et al., 2011). In Romania measurements of LTE1800 and LTE2600 were done in the city of Iasi.

According to the measurements performed for this preliminary survey, the maximal extrapolated E-field values varied from 0.008 V/m to about 3.5 V/m, which is less than 5.5% of the exposure limit (Lunca et al., 2014).

In a practical exposure situation, the effects of simultaneous different NIR frequencies (FM, TV, WIFI and Cellular) are additive. Using Equation (1), the total ER for all points measured is 0.38 below the unity.

Conclusions

Non ionizing radiation levels measured (Electric Fields) in Natal city were below the safety reference levels. The intensity of electromagnetic waves from 18 TV Broadcast stations is higher in 68.6% of the sampled measurement points. TV Broadcast services dominate ER composition even for some points closer to towers of Mobile Telephony. There are some reasons to explain these results: the high power of TV Transmissions (9 to 101 kW ERP in Natal City) and the high technology of Mobile Telephony Transmissions. Most cellular radio systems provide for the use of transmitter power control to reduce co channel interference for a given channel allocation. In this case, the effective power of the Global System for Mobile (GSM) and Universal Mobile Telecommunications System (UMTS) transmissions is dynamic and rationally controlled according to instantaneous traffic of mobile calls and data communications. Cell phone towers are considered as low power installations when compared with broadcast TV (Nworgu et al., 2010).

The highest composed (all services) measured electric field value was 7.78 V/m at P22. Maximum exposure ratios are well below the ICINRP / ANATEL limits for non-ionizing radiations. The highest ER of 4.77 10^{-2} at P22 (TV) is below the unity. More precise assessment about Mobile Telephony radiation must be analyzed with care, such as measurements in points aligned in azimuth and elevation with the base stations' antennas. New field measurements will be necessary to monitor the significant growth of 4G base stations expected for the current and next years.

Conflict of Interest

The authors have not declared any conflict of interest.

ACKNOWLEDGEMENTS

This work is partially supported by FAPERN and CNPq under the scope of covenant 005/2011 PPPIV / number 65, and by UFRN – PROGRAD / PROEX / PROPESQ internal project.

REFERENCES

Agência Nacional de Telecomunicações (2002). Regulamento sobre limitação da exposição a campos elétricos, magnéticos e eletromagnéticos na faixa de radiofrequências entre 9 kHz e 300 GHz. Annex to Resolution n° 303, Brazil.

Brazil (2009). Brazilian Law n° 11.934. [site visited on 2014 Mar. 29]. Avaible from: http://www.planalto.gov.br/ccivil_03/_Ato2007-2010/2009/Lei/L11934.htm.

Bottura V, Borlino MC, Mathiou M, Adda S, D`Elia S, Vaccarono D (2012). Measurements of Electromagnetic Field strength in Urban Environment from UMTS Radio base Stations and Analysis of the Relation with the Radiated Power. Available from: http://ieeexplore.ieee.org/xpl/articleDetails.jsp?reload=true&tp=&arnumber=6396896&queryText%3DMeasurements+of+Electromagnetic+Field+

Eskander EF, Estefan S, Abd-Rabou AA (2012). How does long term exposure to base stations and mobile phones affect human hormone profiles? Clinical Biochem**.** 45:157-161.

Feychting M, Ahlbom A, Kheifets L (2005). EMF and health. Annu. Rev. Public Health 26:165-89.

Gotsis A, Papalikolau N, Komnakos D,Yalofas A, Constantinou P (2005). Non Ionizing Electromagnetic Radiation monitoring in Greece. Available from: http://ikaros.teipir.gr/era/era2/A2/A21.pdf.

International Commission on Non-Ionizing Radiation Protection (1998). Guidelines for Limiting Exposure to Time-Varying Electric, Magnetic and Electromagnetic Fields (up to 300 GHz). Health Phys. 74(4): 494-522.

Lunca E, Damian C, Salceanu A (2014). EMF Exposure Measurements on 4G/LTE Mobile Communication Networks. 2014 International Conference and Exposition on Electrical and Power Engineering (EPE 2014), 16-18 October, Iasi, Romania , P. 545.

Nworgu OD, Anyaeji CA, Osahon OD,Sekegor E (2010). Measurement of radio frequency radiation (RFR) power levels from some GSM base stations. Journal of the Nigerian Association of Mathematical Physics. 17:469–474.

Pérez-Vega C, Zamanillo JM (2005). Measurements of Non-Ionizing Radiation Levels in an Urban Environment. University of Cantabria, Communications Engineering Department (DICOM), Santander, Spain.

Salles AA, Fernandez CR, Bonadiman M (2003). FDTD simulations and measurements on planar antennas for mobile phones. Microwave and Optoelectronics Conference (IMOC). Proceedings of the 2003 SBMO/IEEE MTT-S International. 2:1043-1048.

Tesneli AY, Tesneli NB, Kanberoglu B (2011). Measurements of Electromagnetic Radiation in an urban environment. Available from: http://memberfiles.freewebs.com/14/16/50451614/documents/MEASUREMENTS%20OF%20ELECTROMAGNETIC%20RADIATION.pdf

The Rio Declaration: Principle 15 – the Precautionary Approach. Urban Governance: precautionary principle. [site visited on 2013 Nov. 11]. Available from: http://www.gdrc.org/u-gov/precaution-7.html.